Determination of the influence of machining defects on the magnetic field as a part of the design of new magnets for the CEBAF 12-GeV upgrade

Nicolas Ruiz
Direction: Jay Benesch

Abstract

In order to eventually guide the electrons throughout the accelerator up to their highest energy, the beam trajectory has to be simulated for the entire accelerator with appropriate numerical codes, such as ELEGANT, Optim, etc. prior to the actual facility construction. In the 12 GeV project framework, constraints are tighter than they were for the 6 GeV machine and the accuracy of the simulations have to catch up. Since measured data concerning the elements are not available in many cases, local scale simulations acquire a very particular importance for they can be the only way available to determine the characteristics that will be used to introduce each magnet into whole-accelerator simulations. The present study focuses on a possible improvement of those local simulations by making them take into account more realistic parameters such as machining defects.

The local scale simulation tool used in this study takes a large number of characteristics of the magnets into account. However, none of the simulations realized so far included geometry imperfections. The poles were assumed to be perfectly parallel, their surface to be perfectly plane... Those assumption appeared to be valid up to now, but since both fields and steel saturation in the magnets of the 12 GeV-configured lattice are going to be much higher than in the present 6 GeV machine, the idea of taking geometrical imperfections into account arose from the concern of being able to precisely specify the tolerances that were to be required for the new magnets.

The first models comprising simulations of machining defects are created throughout this study, and a valid perturbation modeling technique is developed. A strong correlation is observed between the first skew multipole terms of the field and the amplitude of the geometrical perturbation and conclusions are drawn concerning the field perturbations induced in the zone located between the magnet poles. However, the mesh densities reached at the time of this study and the field evaluation techniques that were exploited did not allow to draw conclusions regarding the influence of the edges of the magnet poles whose study remains for further work on the subject.

Discrepancies between the actual values of the simulated field perturbations and the measured data that is available are addressed and some advice is dispensed concerning future parts specifications and assembly. The final word however recalls that actual direct measurements of what was simulated are of course desired to qualify the results and the conclusions.

Introduction

This document presents the work realized by the author for his master thesis under the direction of Jay Benesch. It is divided in six main parts.

The two first parts explain the origins of the concern founding this study as well as the strategy that was elected in order to establish conclusive results. The third part relates step by step the proceeding that has been followed, in accordance with the above mentioned strategy. Part four presents the results of the study along with their interpretation. The practical conclusions that can be deduced from those results are listed in part five. References, bibliography and annexes constitute the sixth and last part of this document.

Note: Out of concern for consistency with the scientific procedures being followed among the physicists at Jefferson lab, every value in this document is given in the CGS unit system, unless explicitly indicated otherwise.

Table of contents

I - Initial concern 4
I.1 - Initial situation 4
I.2 - Objective of my work 4
II - Strategy 6
III - Technical description of the study 7
III.1 - Description of the modeling environment 7
III.1.1 - Software resources 7
III.1.2 - Morphing tools 8
III.1.3 - Hardware resources 9
III.2 - Description of the part chosen for the study 10
III.2.1 - Context 10
III.2.2 - Magnet description 10
III.2.3 - Criteria for the choice 11
III.3 - Geometrical specifications of the original part 12
III.3.1 - Concern 12
III.3.2 - Tolerances 13
III.4 - Finding a 'worst' machining case 15
III.4.1 - Concept 15
III.4.2 - Presentation of the model 16
III.4.3 - Perturbations applied 17
III.5 - Field evaluation method 18
III.5.1 - Definition of multipoles 18
III.5.2 - Measuring multipoles 21
III.5.3 - On skew multipoles 24
IV - Results 25
IV.1 - Effect of the introduction of a perturbation 25
IV.1.1 - Presentation of the original model 25
IV.1.2 - Analysis of the perturbed model 25
IV.1.3 - Comparison with a full-height, non-perturbed model 29
IV.1.4 - Comparison with other perturbed models 31
IV.2 - Effect of Field Intensity 33
IV.3 - Quantitative influence of geometrical perturbations 36
IV.3.1 - Models used 36
IV.3.2 - Multipoles behavior 38
IV.3.3 - Relative importance of body and edge fields 42
V - General conclusions 44
VI - References, bibliography and annexes 45
VI.1 - References 45
VI.2 - Bibliography 45
VI.3 - List of Annexes 47

I - Initial concern

I.1 - Initial situation

In order to be able to guide the electrons throughout the accelerator as their energy gets higher and higher, the beam trajectory has to be simulated for the entire accelerator with appropriate numerical codes, such as ELEGANT, Optim, etc. prior to the actual facility construction. This has been done for the 6-GeV current configuration of the CEBAF so that accelerator designers could know in advance where to put the magnets and how to tune them.
To realize the 12-GeV upgrade, a different configuration is required, with new or modified parts, higher fields... The constraints are tighter and the accuracy of the simulations have to catch up.

In whole-accelerator simulations, and because the CEBAF counts more than 2000 magnets, each element cannot be modeled with its entire geometry (coils, steel, current density...). Instead, each element (magnets, filters...) of the lattice is represented by a set of relevant numerical values, like the integrated field 'seen' by the particles traversing it for example, that tells the code how to take into account the influence of this particular element while it computes the beam trajectory. It's a form of multi-scale modeling. Those relevant characteristics must be evaluated for each part, as accurately as possible, since the setup of the whole accelerator depends on it.

The best case occurs when the parts already physically exist and we can make proper measurements of their characteristics. Unfortunately, measurements take time, and the equipment necessary to perform them can be expensive and is not always available. As a result, even in the case of pre-existing 6-GeV parts, many of the characteristics used to simulate the role of these elements had to be evaluated by simulations instead of being actually measured.
Moreover, in the 12-GeV upgrade case, many parts are new or modified, so that their modeling acquires a very particular importance for it is the only way available to determine the characteristics that will be used for their integration into whole-accelerator simulations.

The present study takes place in that context, focusing on a possible improvement of those local simulations by making them take into account more realistic parameters such as machining defects.

I.2 - Objective of my work

As the previous section explained, a series of relevant parameters is determined for each element of the accelerator, either by physical measurement or by simulation of the element's magnetic field on a local scale, for it to represent the modeled element in future larger scale simulations.

The local scale simulation tool used in this study (see section II.3.1.1) takes a large number of characteristics of the magnets into account: the disposition of the coils as well as their current density, the geometry of the return steel, magnetic properties of the steel (editable B-H curve), etc.

However, none of the simulations realized so far with this tool took geometry imperfections into account. The poles were assumed to be perfectly parallel, their surface to be perfectly plane... In other words, no machining or assembly defects were taken into account while defining the geometry of the modeled magnets. Their influence on the field dispensed by the magnet was therefore not present in the results of the simulations, resulting in its not being taken into account in larger scale simulations either.

Since the fields in the magnets of the 12GeV-configured lattice are going to be higher than they currently are, thus placing their steel into a saturated state in many volumes, the idea of taking geometrical imperfections into account arose from the concern of being able to precisely specify the tolerances that were to be required for the new magnets.

The objective of this study is to realize the first models that would take machining defects into account, and to gather information regarding their effect on the magnetic field. Possible results are:

- a better understanding of the current machine and of what has been neglected so far
- a finer notion of the correlation between the mechanical tolerances that lab designers specify for the magnets and the undesired field components that can be expected to arise from those specifications

II - Strategy

The approach that was first decided is the following. All this process is then detailed step by step in the next section (II.3- Technical description of the study).

The first step is to get acquainted with the modeling tool and its morphing functions, in order to be able to introduce geometrical perturbations in pre-existing magnet models.

Then, with the help of my supervisor and according to relevant criteria, a specific magnet in the lattice is selected for geometric perturbations effects on the field to be studied using its model. This election is crucial for the results of this study to be of interest in the design and specification of other magnets.

Once the magnet is chosen and its technical drawing is acquired, design machining tolerances are evaluated. The idea is to start by determining a tolerance-fulfilling 'worst machining case' to work on, to have an order of magnitude of the maximum field perturbation that the current design is allowing. Once again, different scientific criteria are taken into account in this case election, for geometrical product specification intrinsically leaves degrees of freedom in part machining.

Chosen geometrical imperfections are then introduced in the original magnet model. After processing, field calculations reveal, as expected, the apparition of new magnetic field components, that were negligible in unperturbed models.

The next and concluding step of the study is to try and establish correlations between the perturbations introduced and the induced modifications of the field. This paper mainly focuses on the amplitude of the perturbations, and relates discovered relations between magnet machining quality and unwanted field components.

III - Technical description of the study

III.1 - Description of the modeling environment

III.1.1 - Software resources

Magnetic calculations

The numerical code used in this study to model geometries and calculate fields is called Opera 3D. It is written by a British company named Vector Fields [1]. The code has different modules which correspond to the type of physical values one wants to calculate (static or varying electric and magnetic fields, thermal and stress analysis...) and in the present case, the solver used for static magnetic fields is called Tosca.
The scheme for the use of those solvers is the standard pre-processing/solving/post-processing one. Here it is as explained on the company's website:

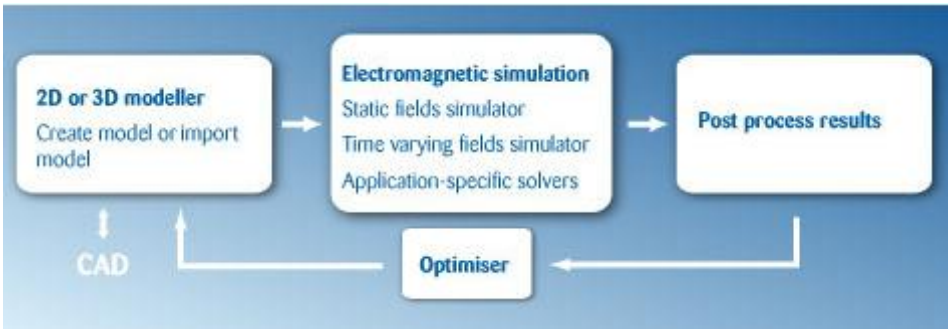

Fig. II.1: Utilization scheme for the Opera 3D numerical code

The most recent pre-processing tool is called the 'Modeller'. It allows you to create 3D volumes and perform simple Boolean operations on them or either import the geometry of your system from another CAD tool. It can also create coils of any shape, and one defines the current that runs through them. In the end, once the required geometry as well as the field sources are defined, a mesh generator based on the ACIS kernel fills the model with finite elements.

Then Tosca, a finite element code, computes the magnetic field in every part of the model using Newton-Raphson relaxation to deal with the steel, whose magnetic properties are non-linear.
An example of a calculation report emitted by the code is available in annex [A4].

Vector Fields
software for electromagnetic design

Fig. II.2: The Vector Fields logo

Post processing

The process used to study the field in the solved models is described in details in section II.3.5. It uses the Opera 3D post processor for initial field evaluations, whose result are treated in spreadsheets [2] [3] afterwards. Those have mathematical and statistical calculation capabilities that are necessary to make the field evaluations exploitable. Their graphical representation functionalities are also very useful when it comes to comparing models, fields...
The data coming out of the post processor is converted into a spreadsheet-friendly format by a Perl script written by the student. An shortened example of a post processor output file as well as the Perl script are available in annexes [A1] and [A2].

III.1.2 - Morphing tools

Since the objective of the study is to take geometrical imperfections into account, it is necessary to get familiar with the options offered by the code that can be used to model such imperfections.
The Opera 3D modeler offers different functions for model distortion.
The main ones are:

- twisting, defining an axe with two points and an angle of torsion

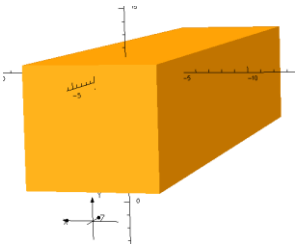

fig. II.3: Original Block used in illustrations

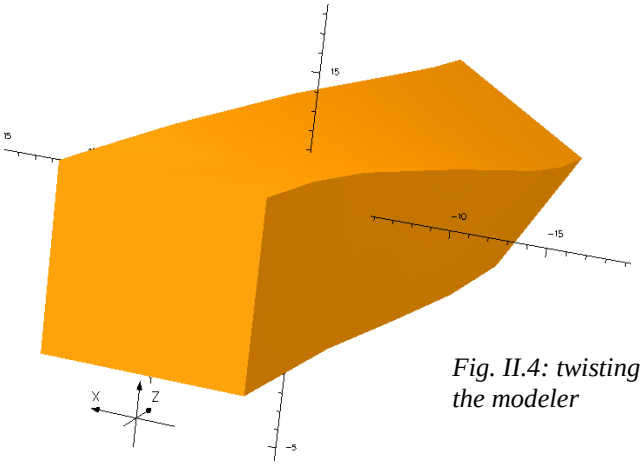

Fig. II.4: twisting operation in the modeler

- stretching, again defining an axe with two points and an axial displacement for each of them

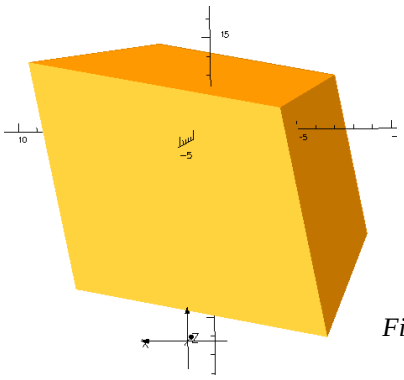

Fig. II.5: stretching illustration

- bending, creating a local coordinate system to define the bending plane, and then choosing an angle and a radius for the bend

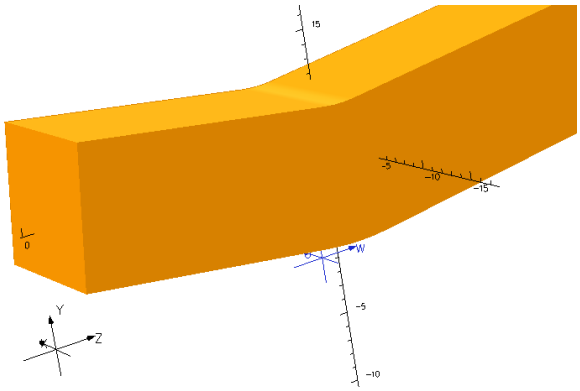

fig.II.6: Bended volume

- the modeler also has a 'general morph' option, which performs any transformation to each of the coordinates, as long as a Cartesian equation is available for that function, which must be properly defined in the treated volume coordinates range.

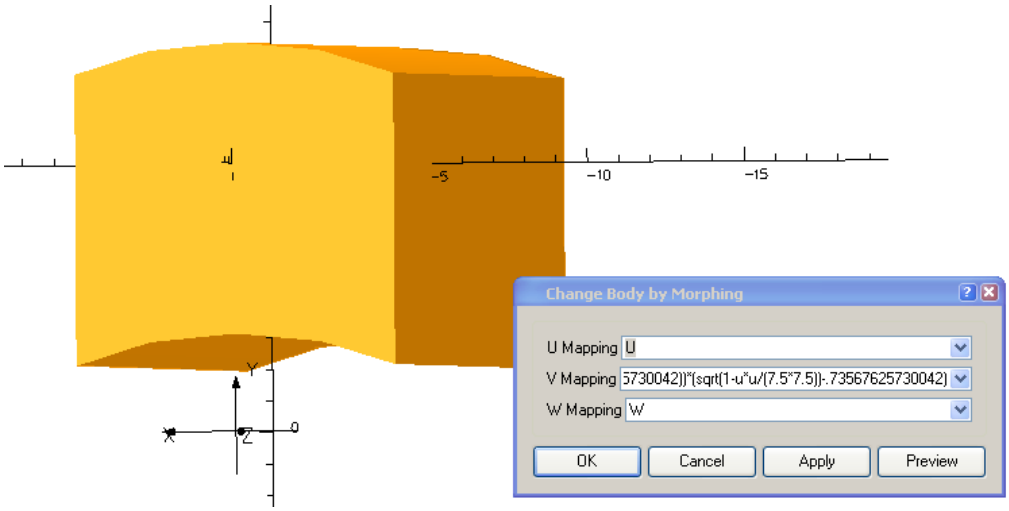

fig. II.7: Example of a general morph. Here the 'Y' coordinate is modified to follow the curve of an ellipse.

III.1.3 - Hardware resources

In order to be able to realize the modeling, meshing and solving operations that this magnetic field fine study requires in good conditions, an appropriate workstation has been used. The calculations made by the student were realized on a machine with the following characteristics:

Make	:	Dell
Model	:	Precision PWS490
Processor	:	Intel Xeon X5355 @ 2.66 GHz (QuadCore)
Memory	:	16 GB of RAM
Operating system	:	Microsoft Windows XP

Professional x64 Edition
Version 2003, Service Pack 2

Apart from these calculation resources, the student was provided with the appropriate means of communication with the other scientists: email, telephone, ...
In addition, the workplace was equipped with a common fax, copier and laser printers.

III.2 - Description of the part chosen for the study

III.2.1 - Context

The 12-GeV upgrade as we have described it from the outside in section I.2.2 has a lot of repercussions on a local scale. As well as some parts are added, others are modified. Figure II.8 shows how some magnets of the spreaders and recombiners will be added some more return steel in order to be able to support more field lines as the field they shall produce in the 12-GeV configuration will drive them into saturation. Figure II.9 shows a prototype.

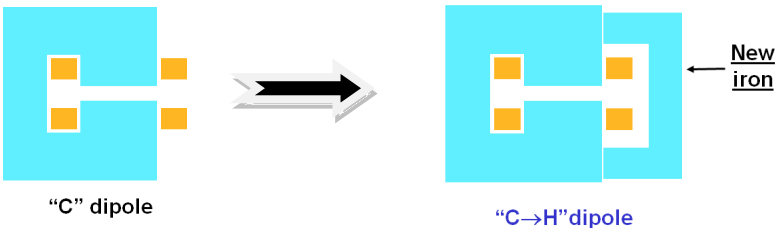

fig. II.8: Schematic representation of the return steel addition in the spreader and recombiner magnets

fig. II.9: Prototype dipole with added H-steel

=> The part elected for this study is one of those extended magnets.

III.2.2 - Magnet description

The current form of the elected magnet has the codename: MAB6R.
'MAB' simply stands for Magnet AB, since the numeration chosen for the magnets is made with letters (AA, AB, AC...). The number '6' indicates that the magnet is situated on the 6th arc, which corresponds to the third pass in the second (western) arc. Finally the 'R' stands for Recombiner, as the magnet is part of the second (see Figure II.10) recombiner. Figure II.11 situates one of the MAB6R magnets. The number '03' is a local numeration, for this very magnet is used several times.

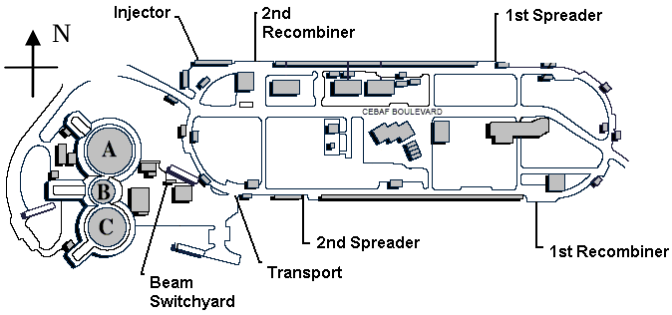

fig. II.10: Scheme of the CEBAF indicating the positions of the spreaders and recombiners.

As the magnet is studied here in its extended form, its name is abbreviated in ABH, where the letter 'H' denotes the fact that this 'C' magnet is somewhat made an 'H' magnet by its being extended. The engineering drawings for the original magnet and its return steel respectively bear numbers 22161-0101 and 22161-0002 [8].

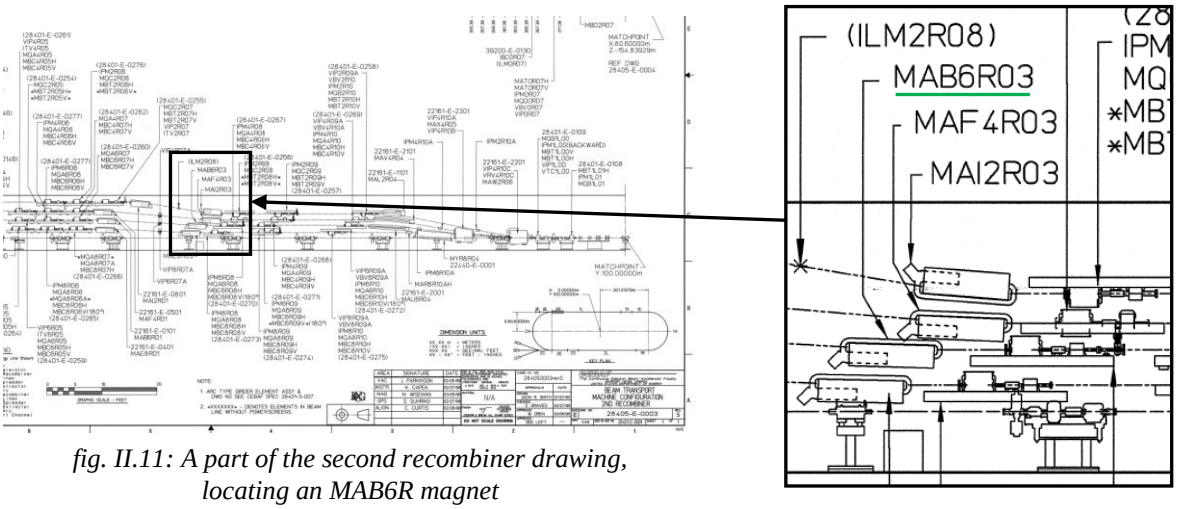

fig. II.11: A part of the second recombiner drawing, locating an MAB6R magnet

III.2.3 - Criteria for the choice

The main criteria that has led to the election of the MAB6R magnet is that once extended to meet the 12-GeV lattice requirements it will be the magnet with the strongest field in the whole lattice (~14kG). It was therefore assumed that any effect of the geometrical perturbations that were to be taken into account in this study would be magnified by the steel saturation.

A couple of other arguments added to this choice's interest:

- the geometry of this dipole is rather abundant, as more than 30 other dipoles in the lattice only differ from it by their current density. Since an evaluation of the correlation between current density and the effects of machining defects enters in this study, the latter gains in application range.

- although quadrupoles are more numerous in the lattice than dipoles (about twice as numerous), the number of magnetic field harmonics measurements available

for them make their study less critical in comparison to the dipoles for which no direct harmonic measurement has been realized so far.

- the reasonable size of the magnet (some of the arc magnets are about three times more voluminous) helps constructing numerical models with reasonable memory requirements, which also enhances the calculation time as well as the pace of the study.

III.3 - Geometrical specifications of the original part

III.3.1 - Concern

The first step in the actual study of the effects of geometrical imperfections on the field induced by the studied dipole is to get familiar with the specifications applied to the latter. Since the 'AB' dipoles haven't been extended into 'ABH' yet, the available data are those relative to the original, non-extended dipoles. It is of fundamental importance to know what the functional surfaces are, as well as the value of the tolerances that were specified for them.

In a dipole magnet, the functional surfaces are obviously the pole tips, where the field lines come out of the return steel to cross the beam trajectory and bend it. The pole tips are the most tightly specified parts since any variation on a pole tip surface directly affects, to an extent that this study is trying to determine, the field seen by the particles and the eventual beam quality.

The steel section is very important too since it determines the maximum magnetic flux density that the steel can support and when it saturates. That is the reason why it was decided that the return steel should be extended for the accelerator upgrade, as explained in section II.3.2. However, a conservative design regarding the steel bulk is cheap enough and sufficient to eliminate the need for a finer study of the section value.

In the case of the pole tips however, there is no limit to the price that a vendor can ask for if the surface quality required is high enough. It is therefore crucial to determine an optimum between the field quality that is needed in the dipoles and the surface quality for the magnet poles that the laboratory is willing or able to pay for.

The object of this study is the extended 'AB-H' magnet, which differs from the currently used 'AB' magnet by its having a thicker return steel section, and thus a higher induced field, but is similar to it in every other dimensional extent.
Let us then examine the specifications that were emitted while designing the current 'AB' magnet.

Figure II.12 and II.13 show the parts of the core detail drawing where the functional surfaces are specified. The full drawing is available in annex [A6].
Note:
All dimensions are given in inches, with a ±0.01 in tolerance if their value is given with two decimals, ±0.005 in if it is given with three.
The full length of the core (37.80 in, implicitly ± 0.01 in) was indicated in another view, not reported here for it held no functional specification.
The following representations have been rescaled to fit the page.

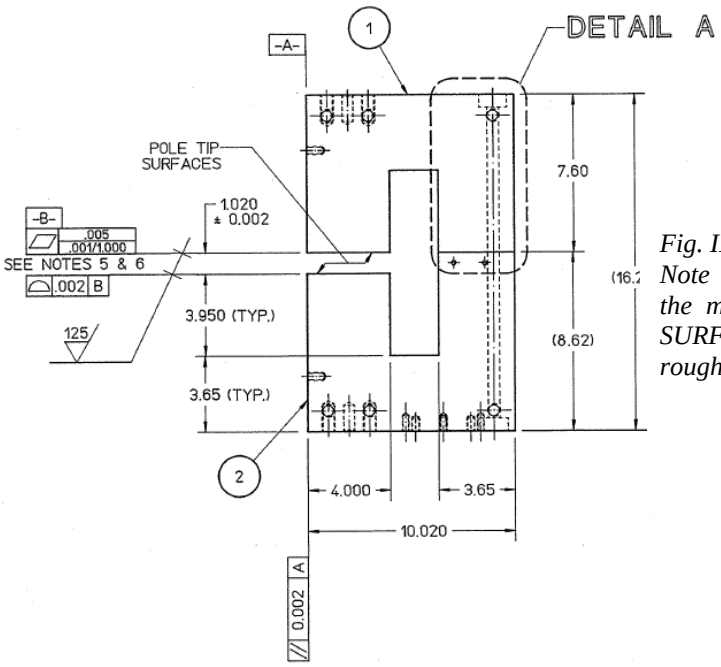

Fig. II.12: Side view of the core of the 'AB' magnet. Note its characteristic 'C' shape. The beam travels through the magnet between the two surfaces marked 'POLE TIP SURFACES' along a path (treated in section II.3.5.2) that is roughly perpendicular to the drawing plane.

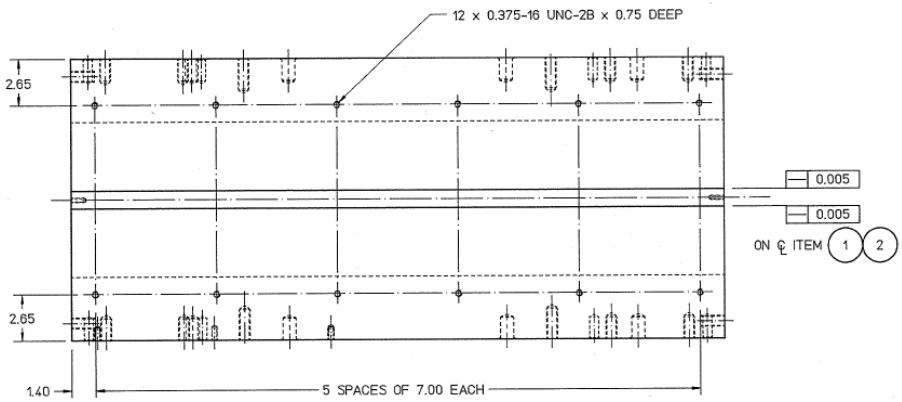

Fig. II.13: Front view of the core.

III.3.2 - Tolerances

Local sizes 1.020 ± 0.002 (see fig. II.12)

This specification requires that any measurement of the gap width in a vertical section plane of the dipole return a value between 1.018 and 1.022 inches.

Flatness -B- .005 .001/1.000 (see fig. II.12)

The specification first names the upper pole simulated datum (theoretical plane associated to the real pseudo-planar surface of the pole tip) 'B'.

Then the upper flatness specification requires that the whole surface of the pole tip be comprised between two theoretical parallel planes .005 inches far from each other.
The lower specification adds to the first one another condition, according to which each 1-in^2 surface on the pole tip must comply with a 0.001-inch flatness tolerance. This helps avoiding local abrupt variations without having to reduce drastically the tolerance for the whole surface.

Profile of a surface ⌓ .002 B (see fig. II.12)

This specification requires that the specified surface belong to a three-dimensional tolerance zone made of two surfaces whose theoretical profile is defined by the datum reference (B in this case) and which are distant from each other by the tolerance value (.002 in here). Since B is a plane, and after broaching the topic with the engineering service, it was concluded that this specification meant that the lower pole tip had to belong to a tolerance zone made by two theoretical planes, parallel to each other and parallel to B, .002-in apart from each other, which is equivalent to a parallelism specification.

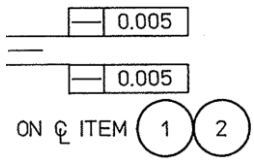

Straightness (see fig. II.13)

According to the authors of the drawing (Annex [A6]), the "℄" indication under the two ⏥ 0.005 specifications indicates that the straightness condition applies to the centerline of each pole tip (See Fig. II.14), in spite of the mention being made of elements ① and ②.

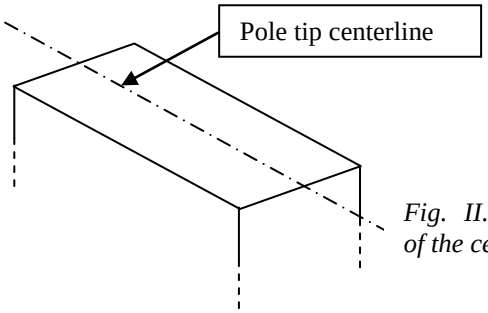

Fig. II.14: Illustration of the centerline notion

The indications regarding the use of the straightness specification found in the literature supplied to the student [4] state: " Straightness tolerance is typically used as a form control of individual surface elements such as those on cylindrical or conical surfaces. Since surfaces of this kind are made up of an infinite number of longitudinal elements, a straightness requirement applies to the entire surface as controlled in single line elements in the direction specified. [...]The straightness tolerance must be less than the size tolerance. "
Since in this case the size tolerance comes to be tighter than the straightness tolerance, it has been accorded that the straightness specification was included in the flatness specification. The former will therefore be ignored henceforth.

//	0.002	A

Parallelism (see fig. II.12)

This specification states that the toleranced surface must fit between two parallel theoretical planes, also parallel to the theoretical datum plane 'A', and 0.002 in far from each other.
The vertical faces of the poles are not functional surfaces to the same extent as the pole tips for they are expected to be tangent to the field lines and therefore not as influent on their action on the beam as the pole tips are. Consequently, this specification will not be exploited in this study, which will therefore focus on the effect of pole tips perturbation.

Surface texture

The surface texture specifications will not be taken into account in this study for the following reasons:

- the dimensions that surface texture specifications deal with are one order of magnitude smaller than the tiniest values used in form specifications. This has a double consequence. Firstly, those perturbations are expected to have a smaller effect on the field than greater scale ones. Secondly, those dimensions reach the limits of our modeling capabilities, so that their being taken into account should be the object of a separate study.
- surface texture defects are expected to be either noise-like (randomly spread over the surface) or periodic (like the mark of milling), in which case the effects of the induced local perturbations would cancel each other as the field is integrated over the beam path to take the whole dipole effect into account (see sections II.1.1and II.3.5.2).

III.4 - Finding a 'worst' machining case

III.4.1 - Concept

Once considered the specifications that were applied to the dipole and the tolerances they expressed, it was decided as explained in the previous section that straightness, vertical parallelism and surface-texture specifications would not be exploited in this study, which would be focused on the flatness of the upper pole, the profile of the lower pole (which was said to be equivalent to its parallelism to the upper pole) and on the local sizes that were specified for the gap.

Modeling operations started with the following concern: now that the tolerances on the critical parts of the dipole are known, the first question that has to be answered is *To what extent is the current design allowing the field to be perturbed from its theoretical value?*

It was then decided to model a dipole that would meet the tolerances, but with a play as low as possible - a 'worst machining case' - whose field, once evaluated, would reveal the nature and order of magnitude of the field perturbations that are being dealt with.

The present section presents the model that was adopted for that function, after a phase of experimentation on modeling possibilities and limitation, along with the perturbation that were applied to it.

III.4.2 - Presentation of the model

Figure II.15 shows an overview of the geometry of the 'ABH' model, realized in the Opera modeler according to the design specifications for the 'AB' magnet and for its steel extension.

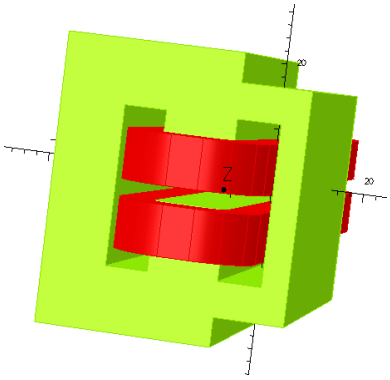

Fig. II.15: Overview of the first perturbed model of the ABH magnet

Since the perturbation applied to the pole tips are of the order of magnitude of the tolerances that were applied to those surfaces (i.e. ~10^{-3} in), they are not visible on an overview of the magnet.

Specific steel magnetic properties were specified (Fig. II.16) for the behavior of the modeled steel to be as close as possible to the steel that is actually used to build the CEBAF magnets.

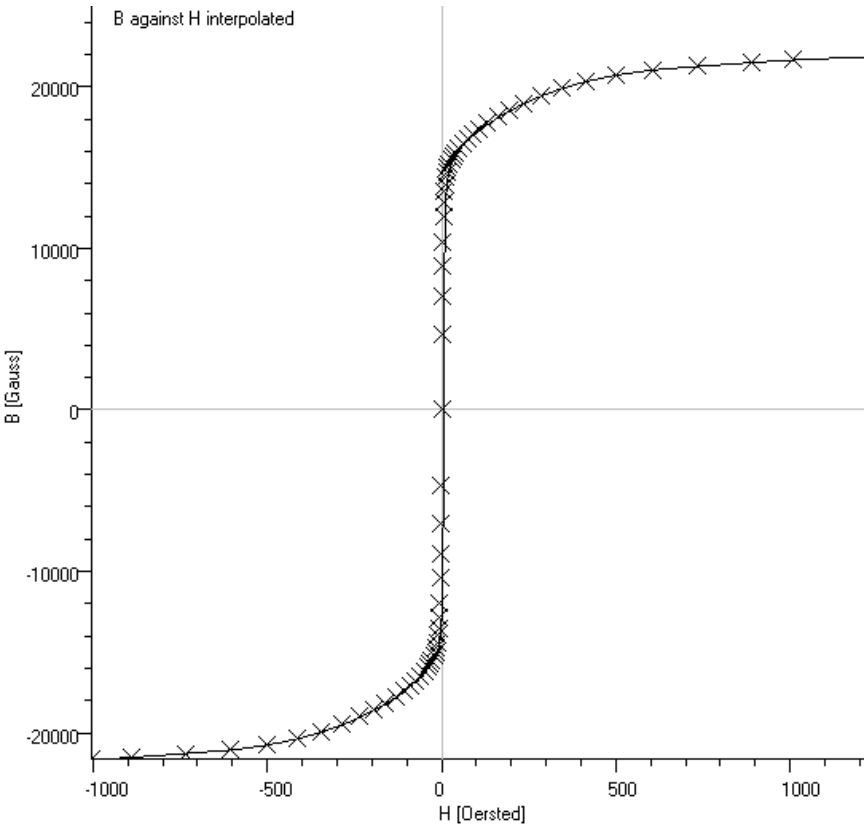

Fig. II.16: B-H curve defining the properties of the steel used in the calculations, obtained from measurements on steel taken on a section of steel from an ingot used in making CEBAF magnets.

III.4.3 - Perturbations applied

This paragraph deals with the perturbations that were chosen to be applied in this model.

Transverse perturbations

Let us consider a transverse plane, perpendicular to the general beam direction, in order to discuss the nature, extent and justification of the perturbations that are perceivable transversally.
Figure II.17 gives a schematic representation of the shape of the perturbed pole tips in a transverse plane.

Since the parallelism tolerance (⌓ .002 B) is a relative property, it was decided that the reference 'B' on the upper pole was going to be modeled horizontally for the parallelism defect to be easily managed by the orientation of the lower pole.

This election implies that the upper pole has a transverse flatness default of 0.002 inches, which is the maximum tolerated since:

- it is only 4 inches wide,
- the flatness default cannot exceed 0.001 in per inch, (-B- ▱ .005 .001/1.000)
- the tangent plane has to be horizontal for the flatness and parallelism defects to be treated separately.

The upper pole flatness defect was at that stage modeled by a parabola, since it was assumed that this convex shape would favor the divergence of the field lines on the sides of the poles, thus magnifying the effect of the tip non-planarity on the field.

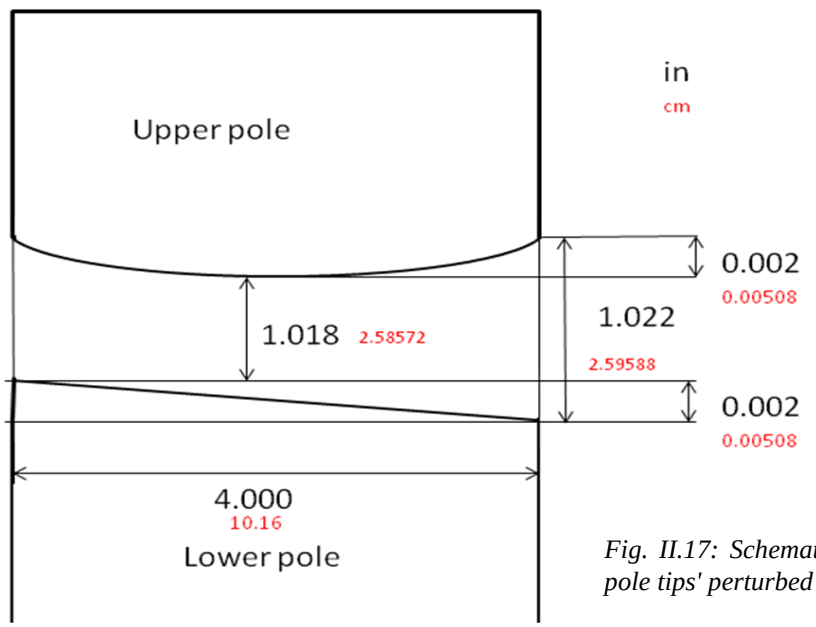

Equations of the slope and parabola:

$$y = \frac{0.00254}{5.08} \cdot x$$

$$y = 1.9685039370079 \cdot 10^{-4} \cdot x^2$$

Fig. II.17: Schematic representation of the pole tips' perturbed shape

The parallelism specification that was applied to the lower pole by means of the profile specification (⌓ .002 B) was taken into account by 'tilting' the lower pole tip with a precisely defined slope so that its tip can be exactly 0.002 inches non-parallel to the upper pole's 'B' reference datum plane: a tangent plane that was made horizontal on purpose, as explained before.
In that configuration, one can verify that the local size specification is verified everywhere.

Longitudinal perturbations

In a first step, it was decided that longitudinal perturbations would not be taken into account, for modeling reasons. In fact, the vertical symmetry of the model was broken by the introduction of the transverse perturbations, which caused the model size, and the calculation time thus, to almost double. Introducing longitudinal perturbations would break the longitudinal symmetry, doubling the solver burden once more. Since perturbed models took around 15 hours to solve, it was decided that the study would start with transversal perturbations only.
From another point of view, the longitudinal axis is parallel to the machining direction, so that most of its defect content is likely to be related with vertical milling marks, which was said to be negligible in the surface texture paragraph of the II.3.3.2 section on tolerances.
In the end, longitudinal perturbations are not treated in this study.

III.5 - Field evaluation method

III.5.1 - Definition of multipoles

Introduction

When an accelerator is constructed, the nominal trajectory of the particle beam is fixed. This trajectory may simply be a straight line, as is the case in linear accelerators. In circular machines such as the CEBAF in its entirety, however, it has a more complicated shape consisting of numerous curves connected by straight sections of various length (the spreaders are a good example of that complexity). The beam follows the resulting path until it is accelerated to the required extent and is sent to the halls. But on another scale, the trajectories of individual particles within the beam always have a certain angular divergence and without further measures the particles would eventually hit the wall of the vacuum chamber and be lost.
It is therefore necessary first of all to fix the beam trajectory, in general an arbitrary curve and then to repeatedly steer the diverging particles back onto the ideal trajectory. The latter, termed the 'orbit', is fixed by the construction of the accelerator, taking numerous parameters into account, such as the energy of the particles, a reasonable steering radius for them given the field strength that can be reached by the magnets and the desired/available size for the accelerator facility... In most general terms, the steering is done by means of electromagnetic fields ($\vec{E}$ and $\vec{B}$) in which particles of charge e and velocity $\vec{v}$ $\boldsymbol{v}$ experience the Lorentz force:

$$\vec{F} = e(\vec{E} + \vec{v} \times \vec{B}) \qquad (2)$$

At relativistic velocities, the effect of magnetic fields is so strong compared to the effect of technically achievable electric fields that those are mostly employed at very low energies.

Decomposition around the ideal trajectory

To describe the motion of a particle in the vicinity of the nominal trajectory, the laboratory frame is not the most appropriate, given the smallness of the beam transverse dimension compared to the radius of curvature of the trajectory. Instead, a local Cartesian coordinate system $K = (x,y,s)$ whose origin moves along the trajectory of the beam is used (Fig. II.18).

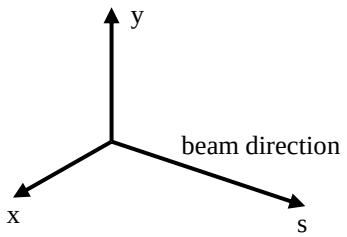

Fig. II.18: Coordinate system to describe the motion of particles in the vicinity of the nominal trajectory

The axis along the beam direction is s, while the horizontal and vertical axes are labeled x and y respectively. For simplicity we will assume that the particles move essentially parallel to the s-direction, i.e. $\boldsymbol{v} = (0,0,v_s)$, and that the magnetic field only has transverse components and so has the form $\boldsymbol{B} = (B_x, B_y, 0)$. For a particle moving in the horizontal plane, through the magnetic field there is then a balance between the Lorentz force $Fx = -ev_sB_y$ and the centrifugal force $Fr = mv_s^2/R$. Here m is the particle mass and R is the radius of curvature of the trajectory. Using $p = mv_s$, this balance of forces leads directly to the relation:

$$\frac{1}{R(x,y,s)} = \frac{e}{p} B_y(x,y,s) \tag{3}$$

There is a corresponding expression for the vertical deflection. Since the transverse dimensions of the beam are small compared to the radius of curvature of the particle trajectory, we may expand the magnetic field in the vicinity of the nominal trajectory:

$$B_y(x) = B_{y0} + \frac{dB_y}{dx}x + \frac{1}{2!}\frac{d^2B_y}{dx^2}x^2 + \frac{1}{3!}\frac{d^3B_y}{dx^3}x^3 + \ldots \tag{4}$$

Multiplying by e/p:

$$\frac{e}{p}B_y(x) = \frac{e}{p}B_{y0} + \frac{e}{p}\frac{dB_y}{dx}x + \frac{1}{2!}\frac{e}{p}\frac{d^2B_y}{dx^2}x^2 + \frac{1}{3!}\frac{e}{p}\frac{d^3B_y}{dx^3}x^3 + \ldots$$

$$= \underset{\text{Dipole}}{\frac{1}{R}} + \underset{\text{Quadrupole}}{kx} + \underset{\text{Sextupole}}{\frac{1}{2!}mx^2} + \underset{\text{Octupole}}{\frac{1}{3!}ox^3} + \ldots$$

The magnetic field around the beam may therefore be regarded as a sum of terms, called multipoles, each of which has a different effect on the path of the particles.

Interpretation

The notion of multipoles is of fundamental importance in order to understand the results of the present study, since most of its conclusions will deal with the extent of a multipole's contribution in the field. This notion has a variety of interpretations, and one should not simply stick to the representation in terms of a mathematical expansion. From this perspective, one should however keep in mind two concepts:

- the behavior of the field components with respect to the distance from the ideal beam trajectory, which is a constant for the dipole, a linear slope for the quadrupole, a square dependence for the sextupole...
- the linear nature of a sum which confers intrinsic independence to the different components of the magnetic field

The different names that are given to the terms of the expansion clearly come from the homonym magnets. In the case of a dipole magnet like the ABH for example, the field lines are straight and parallel between the poles (disregarding edge effects) which means that their density - the magnetic flux density 'B' - is constant, as the dipole term in the expansion was. In a quadrupole magnet, the field lines have the shape indicated in figure II.19. One sees that they get closer and closer to each other as the distance from the center raises, and this density growth is actually linear, as was seen in the 'quadrupole' term of the mathematical expansion of the field.

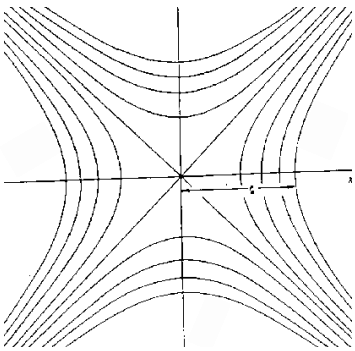

Fig. II.19: Shape of the field lines in a quadrupole magnet

This correspondence between mathematical and physical tools is the basic concept that enables accelerator physicists to build the lattice, the sequence of magnets which constitutes the accelerator along with their set points, so that each mathematical component of the field seen by the particles along the beam path can be managed with a real and concrete magnet type.

III.5.2 - Measuring multipoles

Introduction

As was mentioned in the previous section, the field multipoles have a relatively wide set of interpretation perspectives. In order to understand the way they are measured, treated and compared in this study it is necessary to get acquainted with the cylindrical representation of multipoles.

The mathematical expansion presented in section II.3.5.1 was expressed in a Cartesian coordinate system and the distance from the nominal trajectory was expressed in terms of the abscissa along the horizontal axis *x*. However, the smallness of the beam transverse dimensions compared to the radius of curvature of the trajectory is respected in every direction normal to the trajectory, which confers to the system a cylindrical complexion that is better described in polar coordinates.

The measurement and diagnosis of multipoles underwent somewhat of a revolution around 1965 when J. Cobb and R. Cole used a fast rotating coil to measure quadrupoles at SLAC (Stanford Linear Accelerator Center) in California [5]. The idea is based on the description of magnetic fields in terms of their Fourier harmonic expansion. Picture a coil (Fig. II.20) rotating with constant angular velocity. One side of the coil is placed colinear with the axis of the magnet, the other side sweeps out a circle of constant radius. The voltage seen on an oscilloscope is proportional to the rate of flux cut by the coil. If the magnet is perfect, a perfect sine or cosine wave should be seen at a frequency equal to the revolution frequency for a dipole, twice the revolution frequency for a quadrupole, etc.

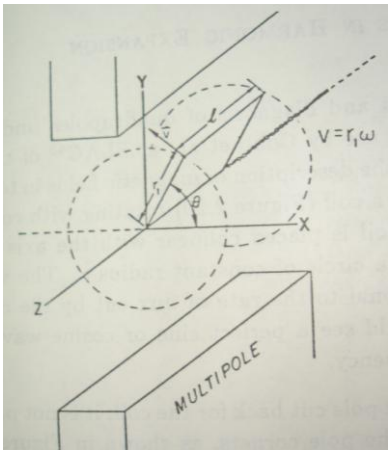

Fig. II.20: Illustration of the field measurement using a rotating coil

The field expansion in cylindrical coordinates is generally expressed:

$$B_r(r,\theta) = \sum_{n=1}^{\infty} K_n r^{n-1} \sin(n\theta - \alpha_n) \tag{5}$$

$$B_\theta(r,\theta) = \sum_{n=1}^{\infty} K'_n r^{n-1} \cos(n\theta - \alpha_n) \tag{6}$$

With the following correspondence:

n = 1	Dipole
n = 2	Quadrupole
n = 3	Sextupole
n = 4	Octupole
n = 5	Decapole
n = 6	Dodecapole or 12 pole

Field evaluation in simulations

The numerical code used in this study [1] to model the dipoles and compute their field has a feature that allows to measure the quality of the field induced by modeled magnets in a way that is very similar to the rotating coil technique, so that it is possible to compare the results of calculations with measured data when available.

In the real measurements that are made at Jlab, the coil is rotated around the beam path as described in the previous paragraph and then moved longitudinally to measure the field along the beam trajectory. As the quantity measured is the amount of flux cut by the coil, all the harmonics are summed and cannot be measured independently. More advanced devices are able to separate the harmonics via a set of multiple dedicated coils.

In the simulated models, the field is evaluated along a circle in a plane normal to the beam trajectory (Fig. II.21). The circle is then displaced along a trajectory that follows the expected beam path - e.g. a circular path within the bending dipole field - and the field is evaluated at each step. A Fourier fit is computed from the circular field evaluation along each circle, simulating the values that would be measured for the field multipoles using rotating coils in a real magnet.

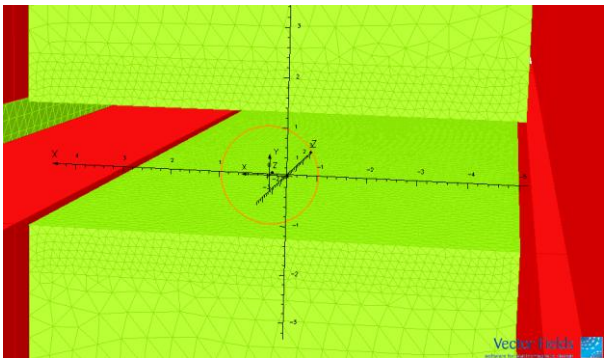

Fig. II.21: Representation of the 1-cm circle around which the fields are evaluated in the simulated models

The script used to generate the circles along the beam path can be found in annex [A3]. The file that is being presented has been shortened for paper economy reasons and only presents the first 5 cm and the last 5 cm of the 75cm-long defined trajectory.
The actual coordinates of the points defining the circles as well as the harmonic values from the Fourier fit applied to the fields evaluated on the circles are given in annex [A1].

As mentioned in section II.3.1.1 - Software resources, the format in which the harmonics are presented in the post processor output file [A1] is quite incompatible with the syntax required for treatment with a spreadsheet editor such as those used in this study [2] [3]. A Perl script, given in annex [A2], was therefore edited by the student to generate a double-entry array presenting the value of each harmonic on each circle all along the beam path.

The circles used to evaluate the 'ABH' magnet models have a radius of 1 cm. This value has been decided upon according to several criteria:

1) The radius cannot be much larger for the magnet poles are only 1.295 cm away from the beam trajectory (and thus from the center of the circle) and a circle evaluating fields too close to the poles would see its evaluation accuracy reduced due to irregularities in the mesh inherent to a change of medium.

2) Since the fields around the circle are evaluated by nodal interpolation, the perimeter of the circle has to be sufficient for the number of finite elements available for the interpolation along the circle to satisfy the sampling theorem.
The Nyquist-Shannon sampling theorem states that:

"If a function *f(t)* contains no frequencies higher than *W* cps*, it is completely determined by giving its ordinates at a series of points spaced 1/(2*W*) seconds apart."

*: Cycles per second - modern unit is Hertz (Hz)

Here the application of this theorem is geometrical instead of temporal: since we are evaluating cyclic functions around a circle, *W* won't be expressed in terms of cycles per second but in terms of cycles per perimeter of the circle. Since the multipoles are evaluated up to the 20-pole (which is then the one with higher frequency), *W* here is 10 cycles per perimeter. For a 1-cm radius circle, the perimeter length is about 63 mm. Therefore, the field has to be evaluated at least every each 1/(2*W*)*63 mm = 3.15 mm. Since in the models studied the mesh size is 2.5 mm in the gap, the sampling theorem is verified with a 1-cm radius circle.

3) Equations (5) and (6) show that each 2n-pole term is proportional to r^{n-1} so that even evaluations made with a large circle can eventually lead to an evaluation at a beam-radius scale.

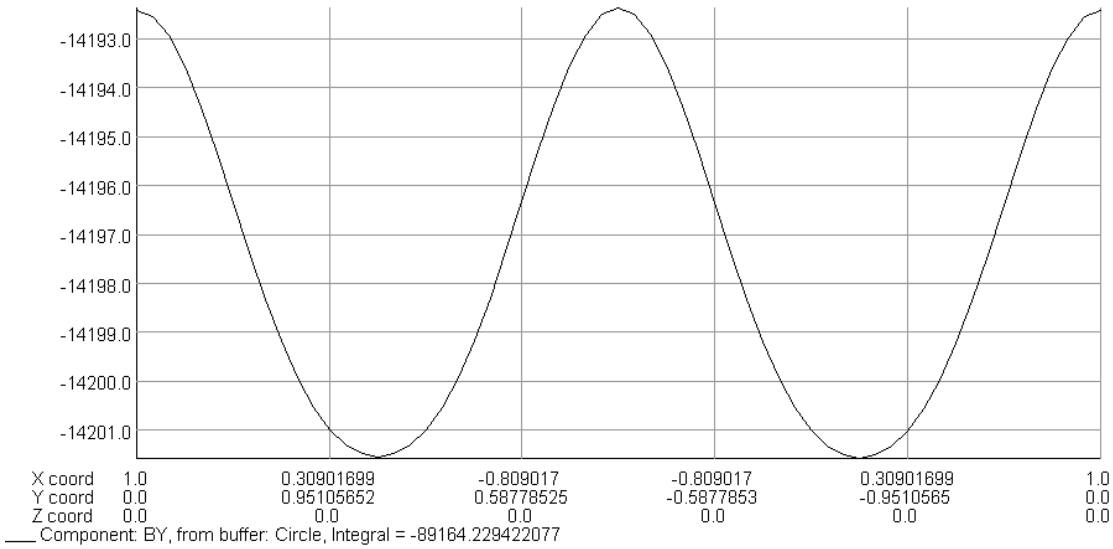

Fig. II.22: Field evaluation around a 1-cm radius circle situated in the center of an unperturbed model of the 'ABH' Dipole. One can clearly see the cosinusoidal shape that was mentioned in the introduction of this section.

III.5.3 - On skew multipoles

Before the research proceeding goes on with the presentation of the first results in the next section, a few precisions about field multipoles should be considered in order to clearly understand those results.

We have seen in the previous section that the field induced by a perfect $2n$-pole magnet could be described as a theoretical say, cosine wave. Basic notions of trigonometry tell us that a rotation of $\pi/2n$ of the coordinate system implies that a term be expressed with a sine if it had a cosine and vice versa. This has a very important repercussion on the practical field for it implies that the field of a perfect $2n$-pole magnet can be described by, say, a sine wave in only one coordinate system or in other words, that in a given coordinate system, we generally need both sine term and cosine term to describe the field content at any given order n because of the angular degree of freedom around the longitudinal axis.

In reality, magnets are never perfectly vertical or perfectly horizontal. There is always a component of the field that is not aligned with the reference, intrinsic to the magnet mis-orientation. Moreover, as the fields induced by the magnets are never quite perfect, even in their own coordinate system, the terms representing 'tilted' content - which are called the *skew terms* - help the accelerator scientists to describe unwanted components of the magnetic field.

IV - Results

IV.1 - Effect of the introduction of a perturbation

The goal of this section is to obtain a first look at the effect that the introduction of a geometrical perturbation in the numerical model of the studied dipole has on its field. For this purpose, the 'Worst Machining Case' (WMC) model, defined in section II.3.4, will first be compared to the original, non-perturbed model that is currently being used to simulate the 'ABH' magnet in the accelerator simulations (cf. II.1.1).

IV.1.1 - Presentation of the original model

From now on, the models will be described in a coordinate system in which the origin is placed in the center of the gap (equal distance from the pole tips and from their borders), *z* is the longitudinal axis and *x* and *y* the transverse directions respectively parallel and normal to the pole tips.

As section II.3.2 explained in details, the 'ABH' magnet is a 'C' shaped magnet that was extended to a pseudo 'H' shape to support superior magnetic flux density. Since the model being used currently to simulate the field that is induced by this magnet is not perturbed, the steel geometry in it has two planes of symmetry: the $z = 0$ and $y = 0$ planes. Consequently and for computation time reasons, the model that is really being solved in non-perturbed calculations only includes the $\{z > 0, y > 0\}$ quarter of the steel. Figure II.23 presents this model along with another one that includes the whole geometry but which is never used for calculations.

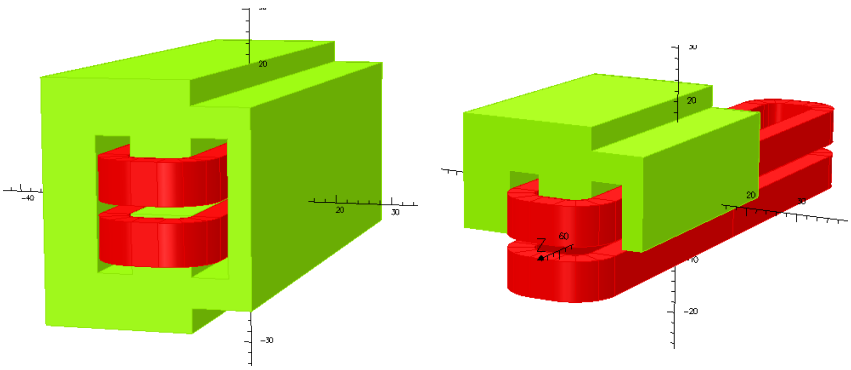

Fig. II.23: Two models including: the full geometry of the steel (left), only one quarter (Right)

In the perturbed WMC model, only the symmetry with respect to the $z = 0$ plane is conserved since the poles are not perturbed equally.

IV.1.2 - Analysis of the perturbed model

The multipole terms of the field expansion (II.3.5) increase with the distance *r* from the beam orbit with an order r^{n-1}. Since the beam transverse dimension is small compared to the magnet gap, with core Gaussian under 0.6 mm sigma throughout [6], the orders for

n > 2 will be neglected for now in front of the two first terms. Since the dipole skew term is null and its normal (not skew) term is easily taken into account in real measurements given its direct effect on the beam trajectory, only the quadrupole term is going to be taken into account at first.

Observations

Figure II.24 and II.25 show respectively the cosine and sine term of the quadrupole harmonic of the field that is 'seen' by the beam along its trajectory in the magnet.

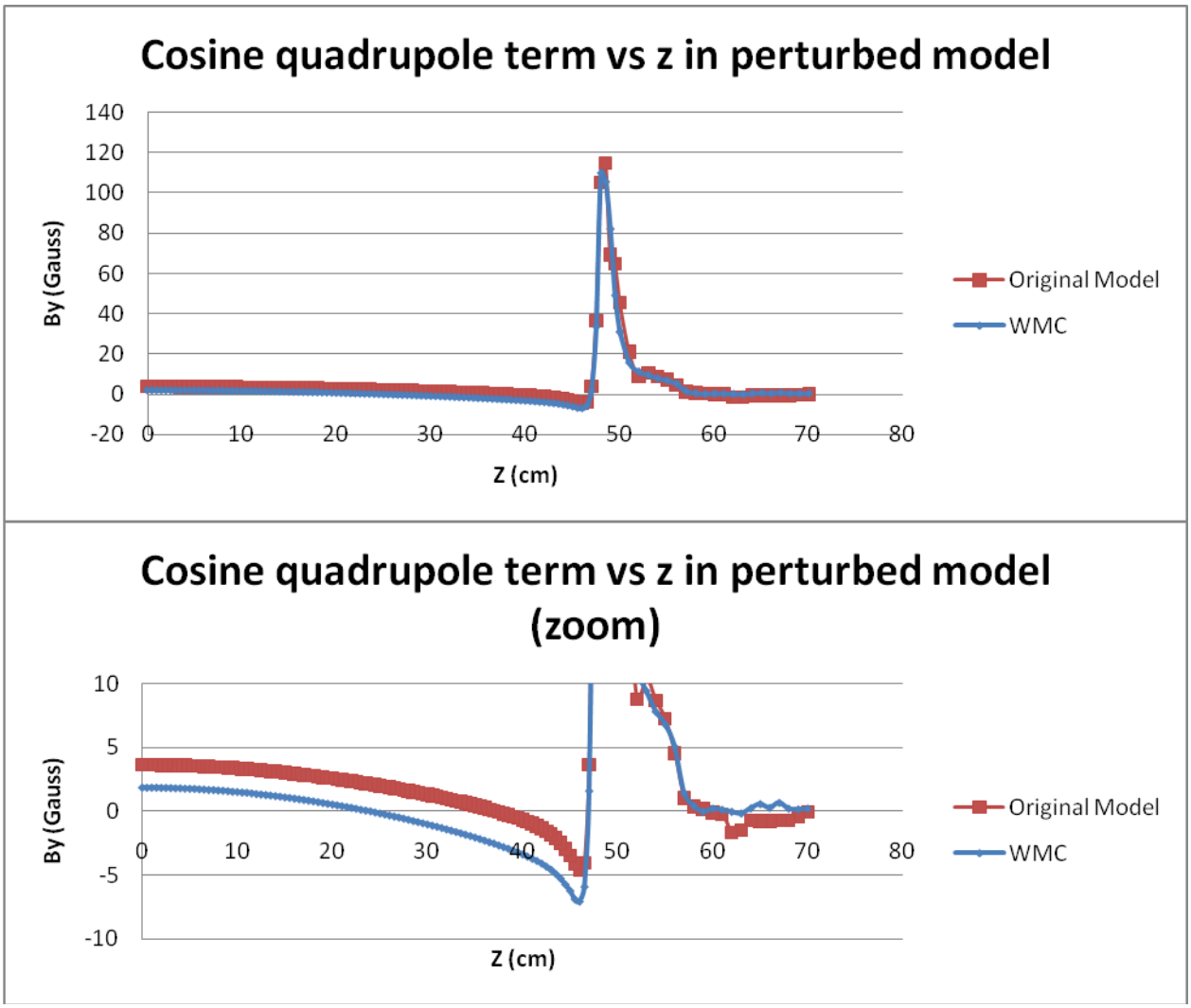

Fig. II.24: Cosine quadrupole term evaluated along the beam path in both the 'Worst Machining Case' model and the original non-perturbed model.

As was explained in the paragraph introducing the coordinate system, the origin is situated in the center of the gap and *z* is the longitudinal axis. Since the models present a symmetry with respect to the *z* = 0 plane, only the *z* > 0 part of the graphics is presented, the other part being identical and in the opposite direction.
The steel body of the magnet ends at *z* = 48.006 cm (37.8 in).

One can see a slight offset in the cosine term value while the beam is still between the poles, but since the tendency is not modified and the lattice is equipped with numerous normal 'cosine oriented' quadrupole magnets, this effect is easy enough to correct for this study not to focus on it.

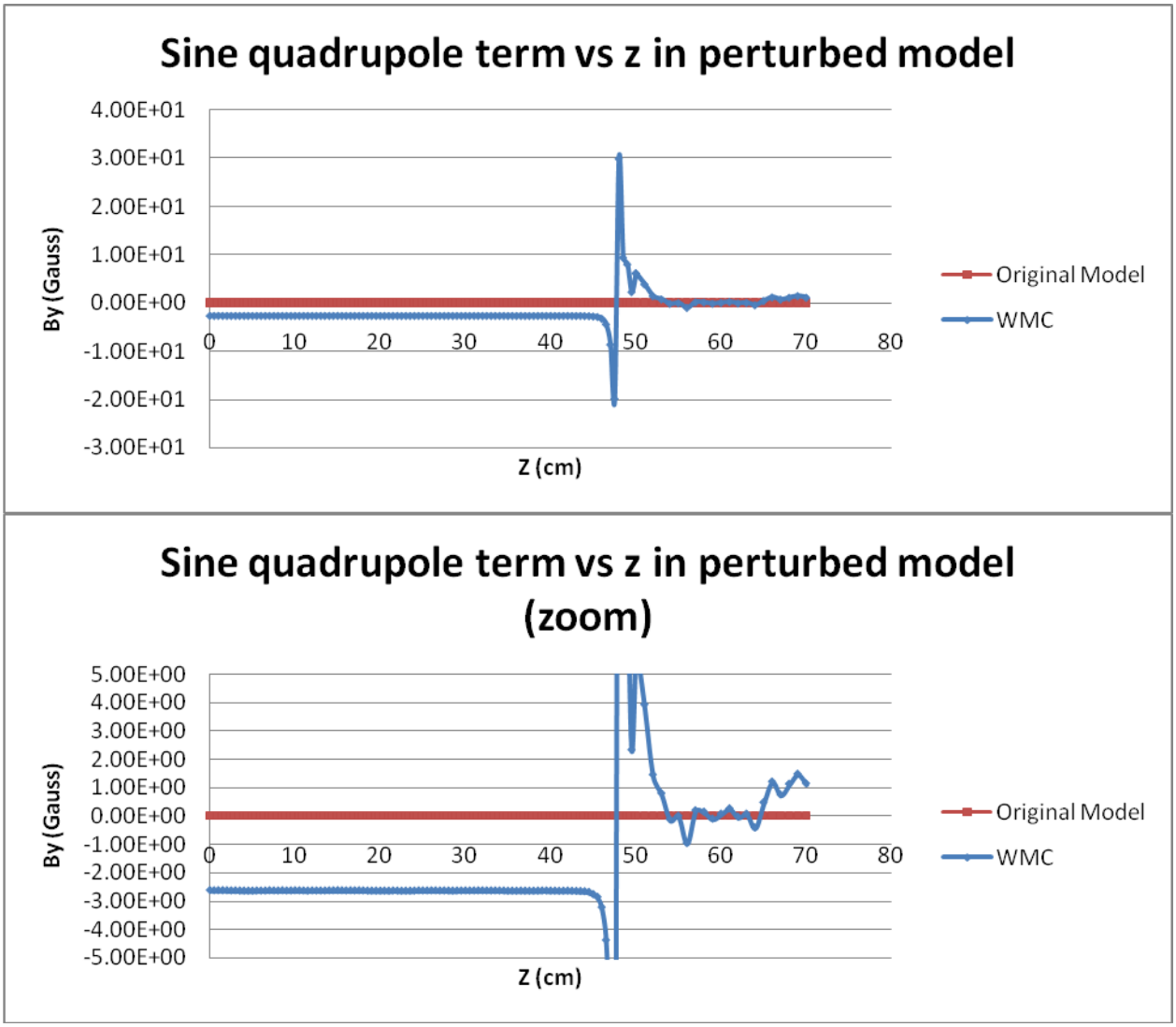

Fig. II.25: Sine quadrupole term evaluated along the beam path in both the WMC model and the original non-perturbed model

Several interesting phenomena are observed here. While the non-perturbed model had all its skew terms artificially set to 0 for the magnet mid-plane ($y = 0$) was a boundary for the model (and thus the boundary condition stated that the field lines had to be normal to the mid-plane), the perturbed model, in which this symmetry is broken, shows:

- a constant body term of several Gauss
- a peak at the end of the steel, one order of magnitude higher than the body value

Comments

As was explained before, the lattice is supplied with numerous normal quadrupole magnets, so that the normal quadrupole perturbation is not much of a problem for it can be corrected easily. On the other hand, skew quadrupole magnets are rare and most of them are situated in the linacs, already set to compensate for the skew terms introduced by the imperfect superconducting RF cavities. There are only two skew quadrupoles in the CEBAF outside the linacs, in the eighth and ninth spreaders. These are used to compensate for all the accumulated error outside the linacs, which represents an equivalent of over 600 cumulated meters of dipole length before the ninth spreader. They are set to reduce x-y coupling to the part per thousand level in the succeeding arc. Typical values are 500-800 G - which is roughly equivalent to 1 Gauss per meter of dipole. Dipole values are about 40% of those considered in this work (see section II.4.2), so 2.5 G per meter of dipole would be typical in the upgrade if disassembling the dipoles to modify the coils and reassembling with H steel do not alter performance.

First normal multipoles are useful: dipoles are used to steer the beam, and quadrupoles to focus it for example. But skew multipole terms play an important role in beam deterioration throughout the accelerator. At 6 GeV the distribution of the particles in the beam transverse dimension is Gaussian and the beam diameter is easily kept under 0.2mm sigma (core Gaussian) [6] throughout. Halo with a quadratic (not Gaussian) transverse profile is sometimes introduced accidentally in the injector and interacts with higher multipoles throughout the machine. As the energy raises (the upgrade purpose is to double it), the synchrotron radiation becomes significant in the arcs and to the initial distribution is added a halo even without injector error. Again, this halo is a quadratically-distributed noise zone around the Gaussian that increases the beam transverse dimension. As was seen many times before, multipole terms get higher with the distance from the center of the beam and as the beam transverse dimension increases, so does its sensitivity to multipole effects. Beam section increase and sensitivity to skew multipole content are two parasite phenomena which favor each other.
Since there are hundreds of dipoles in the lattice, their introducing a hitherto neglected skew term must be studied in details.

Proposal

At this point of the study, it appears clearly that modeling the magnets using only a quarter of the steel for symmetry reasons was too bold an assumption. However, we don't know yet to what extent the skew terms observed in the perturbed model are due to full-height steel modeling or to the actual perturbation.

The next step should therefore be to compare our perturbed model to an unperturbed model comprising the full height of the steel, thus getting rid of the boundary condition that zeroed all skew content of the field in the previous simulation.

IV.1.3 - Comparison with a full-height, non-perturbed model

Figure II.26 shows how the full height of the steel is comprised in the non-perturbed model that is going to be used henceforth, while the longitudinal symmetry that allows us to keep calculation time reasonable is still conserved. Quarter-steel models took roughly half the time half-steel models take to solve, which means that the calculation time passed from around 6-7 hours to around 15 hours. One should keep in mind that each of the simulations presented in this study is the result of several hours of modeling and meshing in the case of perturbed models, plus one night of calculation on a general basis.

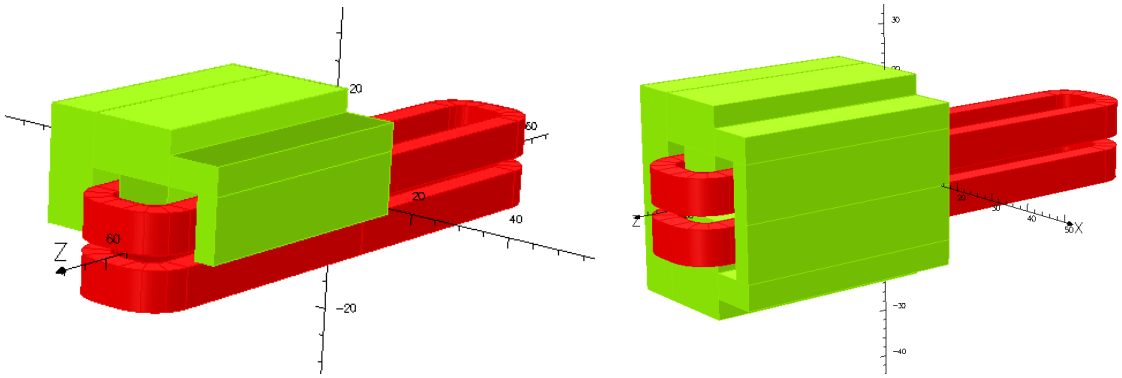

Fig. II.26: 3D representation of the two unperturbed models, respectively assuming a double symmetry (left), or only one longitudinal symmetry (right).

One can observe on figure II.27 that:

- the ~3 Gauss shift in the zone between the poles is conserved
- the unperturbed model now shows a bunch of peaks in the pole edge whereabouts

Interpretation

Although the end of the pole tips are likely to have an influence on the field, the high frequency peak shape that is observed is very unlikely to have any physical relevance. These oscillations are more probably caused by the insufficient mesh density outside the gap zone. While the finite element size is 2.5 mm in the gap, it changes to 5 mm when the beam gets out of the magnet. Although this edge effect is interesting, the study will first focus on the body field whose calculation is more reliable for now (cf. II.3.5.2).

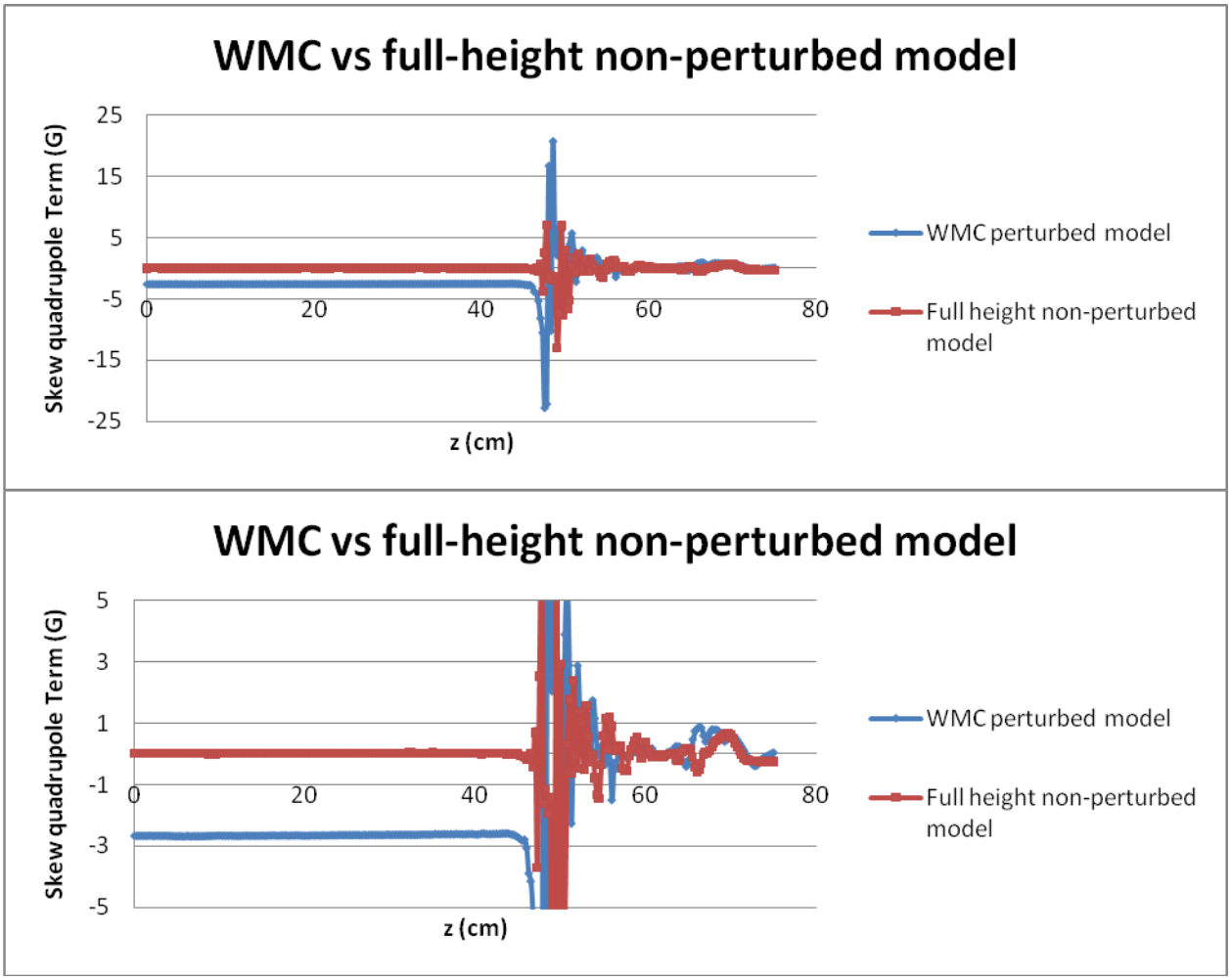

Fig. II.27: Skew quadrupole term evaluated along the beam path in both the WMC model and the full-height non-perturbed model

Proposal

After the influence of the perturbation is confirmed by the comparison with other models, perturbed to the same extent but with different shapes, the study should focus on the determination of the correlation between the amplitude of the perturbation and the extent of the skew quadrupole term. In reality, the magnets will probably not have exactly the non-planarity that has been assumed in the WMC model. It would therefore be interesting to be able to evaluate the field defect that is to be expected from a given planarity of the pole tips.

IV.1.4 - Comparison with other perturbed models

Presentation of the other perturbed models

Figure II.28 presents the shapes that were used to perturb the Test1 and Test2 models. They were mostly chosen to test asymmetric and non-linear shapes, without taking into account their being realistic or not for the moment.

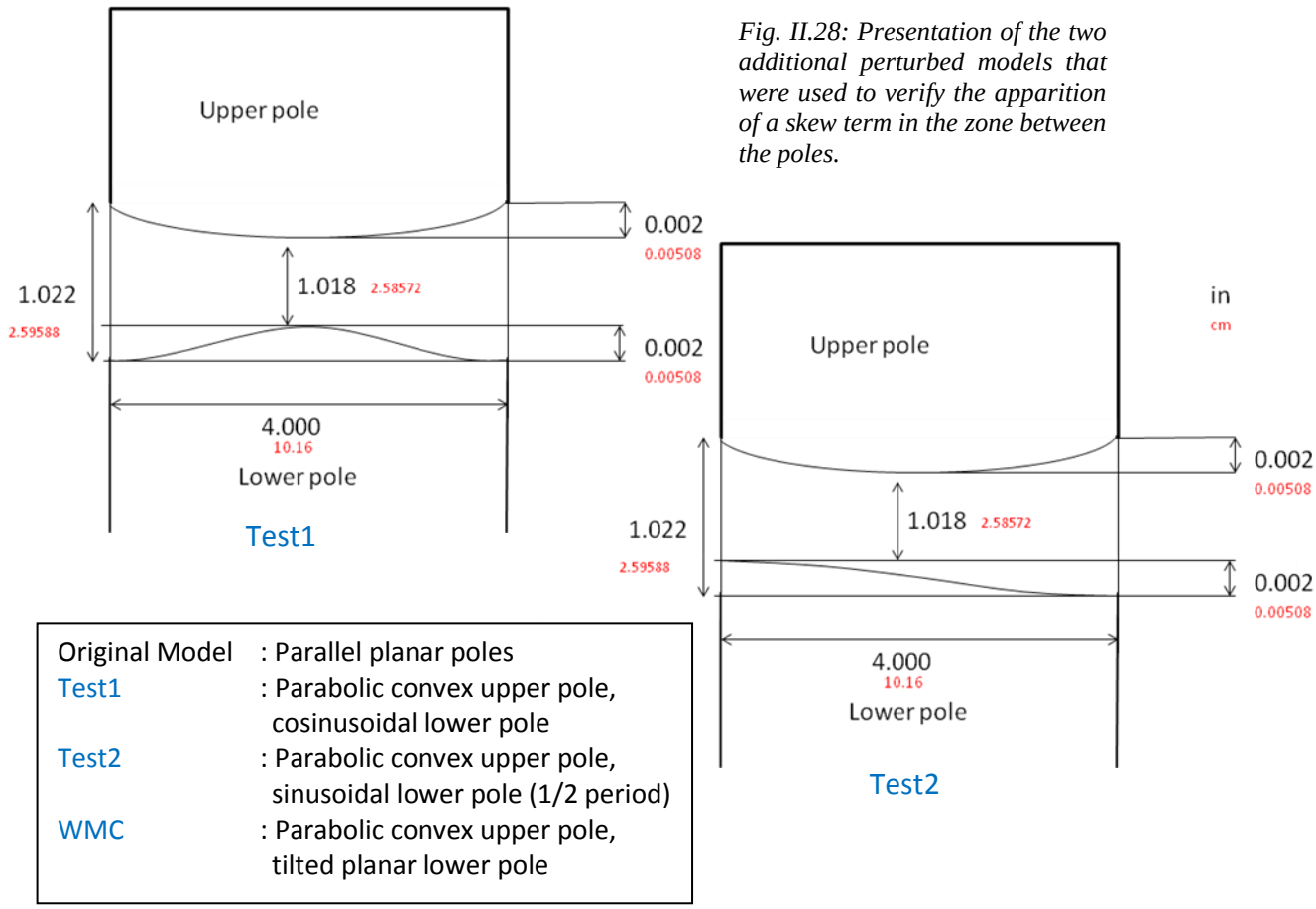

Fig. II.28: Presentation of the two additional perturbed models that were used to verify the apparition of a skew term in the zone between the poles.

Observations

Figure II.29 shows that a skew term is observed in each model and that they all have very similar values, although the sign is opposed in Test1.

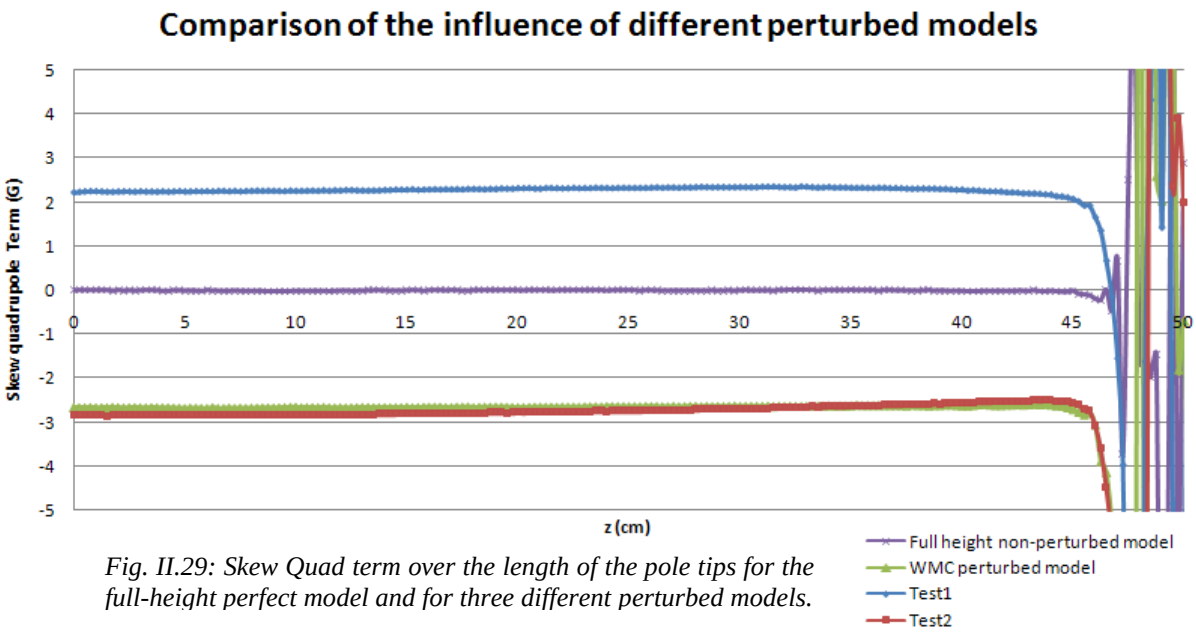

Fig. II.29: Skew Quad term over the length of the pole tips for the full-height perfect model and for three different perturbed models.

Conclusions

It is now confirmed that the geometrical perturbation of the poles creates a skew quadrupole term in the gap of the dipoles. Its sign seems to be related to the relative symmetry of the perturbations.

The arguments that led to decide upon a convex parabola and a tilt for the WMC model were more mathematical than practical:

- the convex shape was assumed to favor the divergence of the field lines
- the tilt was intended to introduce asymmetry and it represented the non-parallelism of the poles.

Although the pole tips are indeed very likely to be somewhat non-parallel in reality, the convex shapes that those models present are very unrealistic on the contrary.
When a surface is milled vertically, the two main causes for shape defects are the orientation of your mill and the quality of the guiding. Since the latter only has a longitudinal effect that is not taken into account in the present study, let us focus on the former:

- if the mill is tilted with respect to the longitudinal axis, the machined surface, as planar as it may be, will end up being tilted by the same amount
- if the mill is tilted with respect to the transverse axis, the machined surface will be a concave ellipse instead of a plane

Since the apparition of a tilt or an ellipse instead of a plane is independent from the sign of the mill orientation defect, one can conclude that those form defects are *always* going to be present on the pole tips, to some extent.

Proposal

Now that the influence of geometrical perturbations has been qualitatively established, the next step in the research progress will be to determine quantitatively the correlation between the amplitude of the geometrical perturbation and the amplitude of the induced field perturbation.
A model presenting a concave ellipse and a tilt should be used for this purpose.

IV.2 - Effect of Field Intensity

Before the research process goes on with the quantitative study of the influence of geometrical perturbations on the field, a parallel study whose purpose is to verify an initial assumption will be presented.

Initial assumption

As section II.3.2.3 stated, the 'ABH' magnet was chosen for this study because it was going to induce the strongest dipole field in the 12GeV-set lattice (~14kG). It was assumed that the steel saturation occurring at those fields would favor field defects and make the study more easily readable.

Verification process

To verify this assumption, it was decided that the initial perturbed model would be solved using different current densities in order to see the tendency of the field perturbation with respect to steel saturation. Since the magnet is never going to be used with higher current than its 12-GeV nominal current I, it was decided that the model would be solved for the following values of the current: $.25I$, $.375I$, $.5I$, $.625I$, $.75I$, $.875I$, I (already solved).
Figure II.30 presents the results of these calculations. A unique value that would represent accurately the field in the gap of each model was needed. Since the previous section showed that the quadrupole term of the field was rather constant far from the edges, an average of the skew quadrupole term of the field was computed for each model over the $z = 0$ to $z = 20$ cm portion of the beam trajectory.
With an average around 15 h of calculation time for each model, solving them all took a little more than 100 h.

Observations

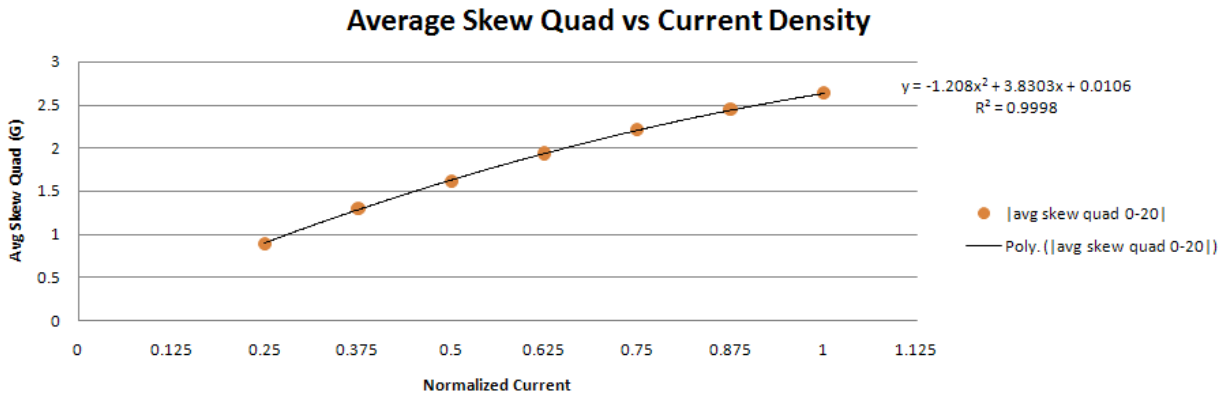

Fig. II.30: Average skew quadrupole term of the field in the center of the WMC model for different values of the current density in the coils

It can be observed that as one would expect the value of the field increases with the current intensity , but the skew quadrupole seems to be attenuated as the current raises which would undermine the hypothesis according to which steel saturation would favor field perturbation. To see better the influence of perturbation on the skew quadrupole content, the average skew quadrupole has been normalized by dividing it by the average normal dipole term of the field (calculated between $z = 0$ to $z = 20$ cm too). The plot is presented in figure II.31 with two different vertical scales.

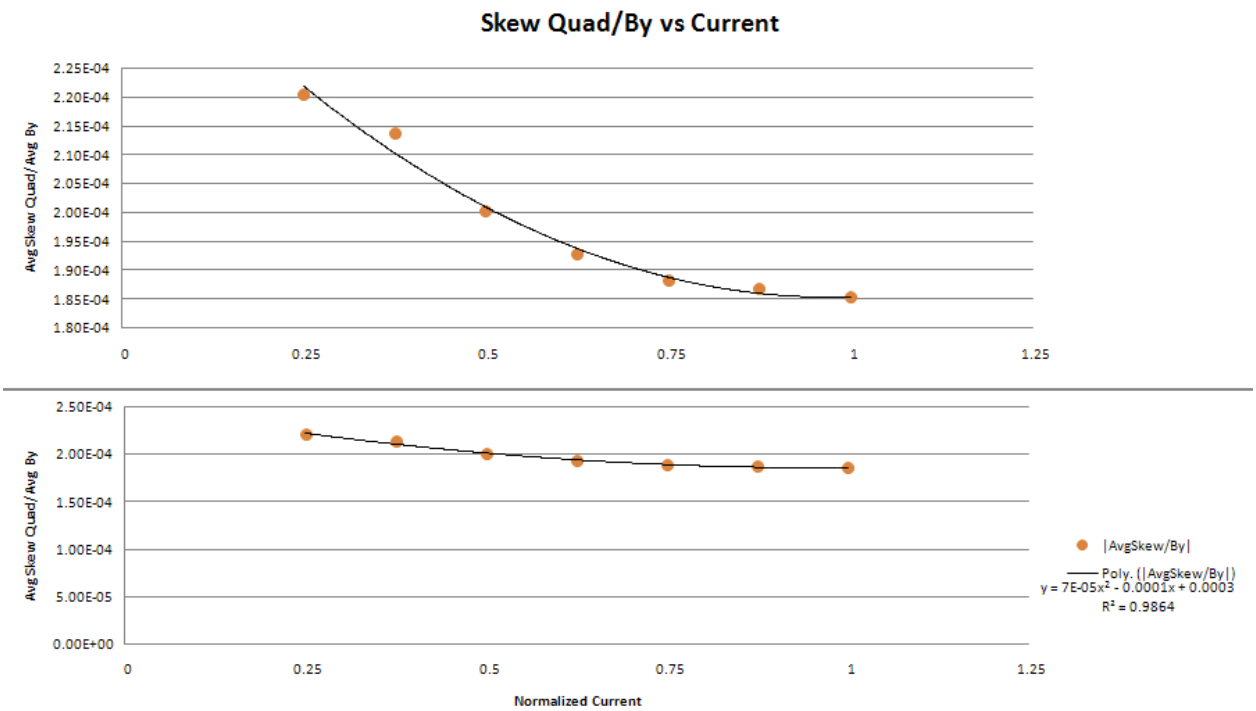

Fig. II.31: Average skew multipole term of the field divided by the average normal dipole term in the center of the magnet gap versus normalized current density

One can see clearly that the relative importance of the skew multipole term with respect to the functional steering field decreases as saturation raises.

Interpretation

This decrease of the relative importance of the skew multipole means that as the magnet is used with higher and higher currents, it becomes relatively less sensitive to the geometrical defects of its poles.
This can be interpreted considering the nature of the saturation phenomenon. As the current augments in the coils, the magnetic field induced in the steel grows. This means that the magnetic flux density increases, that the density of field lines guided by the steel increases. When the steel starts to saturate, its permeability decreases and it admits less and less additional field lines. Since the flux generated by the coils raises anyway, the field lines start to be driven by the air instead of being sucked by the steel. The magnet starts to be less and less 'iron-dominated'.
As the air drives more and more flux compared to the steel, its influence on the field shape gets more and more important. Since geometrical perturbations of the pole tips only affect the field lines that are driven by the steel, one can understand the decrease of their relative influence with the decrease of the relative influence of the steel on the field shape.

Conclusion

The initial assumption regarding the help that steel saturation would provide in studying the influence of geometrical perturbations was wrong, as its effect is actually to lower their influence. However, since this effect is limited to ~20% of the studied value (Fig. II.31) and since this saturation influence verification was being undertaken in parallel to the rest of the perturbation studies, it was decided that the studies should keep using the ABH magnet. One can later translate the results to weaker magnets using the established curves.

IV.3 - Quantitative influence of geometrical perturbations

The purpose of this section will be to look for an exploitable correlation between the amplitude of the geometrical perturbations and their expected effect on the field components.

IV.3.1 - Models used

Presentation

As section II.4.1 explained the convex shapes that have been used to model the perturbations until now are not realistic. As a consequence, the models that are going to be used from now on will have perturbations whose shape can logically be expected from machining defects. It was established that, to some extent, any milled surface is tilted and presents a concave elliptic shape. This is therefore the way in which perturbations will be modeled. However, and although each pole tip should present both a tilt and an concave elliptic shape, those defects will be separated in order to be able to quantify their amount more clearly. This separation will be done artificially by using models that present a concave elliptic upper pole, and a planar tilted lower pole.

The first model created that way was intended to be an equivalent of the WMC model in the way that it was modeled to fulfill the tolerances with a play as low as possible. Nevertheless, since the objective was not to match the tolerances anymore but to make a model that could be easily modified to study different values for the perturbation, this model was dimensioned with metric units, having a perturbation amplitude of 50 microns, versus 0.002 in for the WMC model. The 0.002 in value came from the drawings edited by the engineers, who use the U.S. customary unit system on a general basis, and the 50 microns value was intended to be a starting point for a set of simulations with different perturbation amplitudes that would be realized in a metric system scientific environment (numerical codes, internal communication...).

Figures II.32 and II.33 respectively present the new elliptic and tilted model and the WMC model, for comparison.

Equations of the slope and ellipse:

$$y = \frac{P}{10.16} \cdot x$$

$$y = \frac{P}{1-.7357} * \left(\sqrt{1-\frac{x^2}{7.5^2}} - .7357\right)$$

$$\mathrm{P} = \mathrm{Perturbation\ amplitude}$$

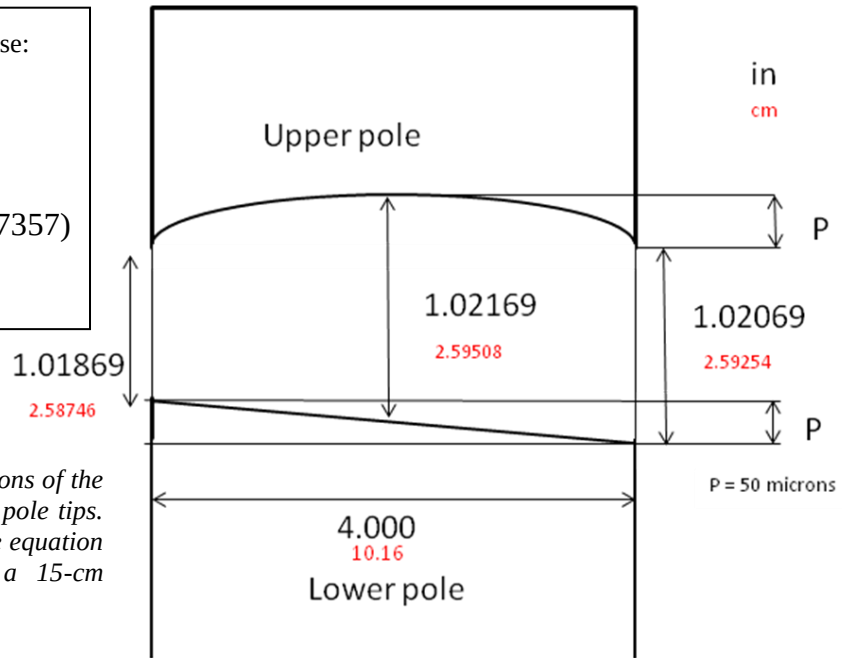

Fig. II.32: Dimensional specifications of the first model with elliptic and tilted pole tips. The numerical values in the ellipse equation come from the assumption of a 15-cm diameter for the mill.

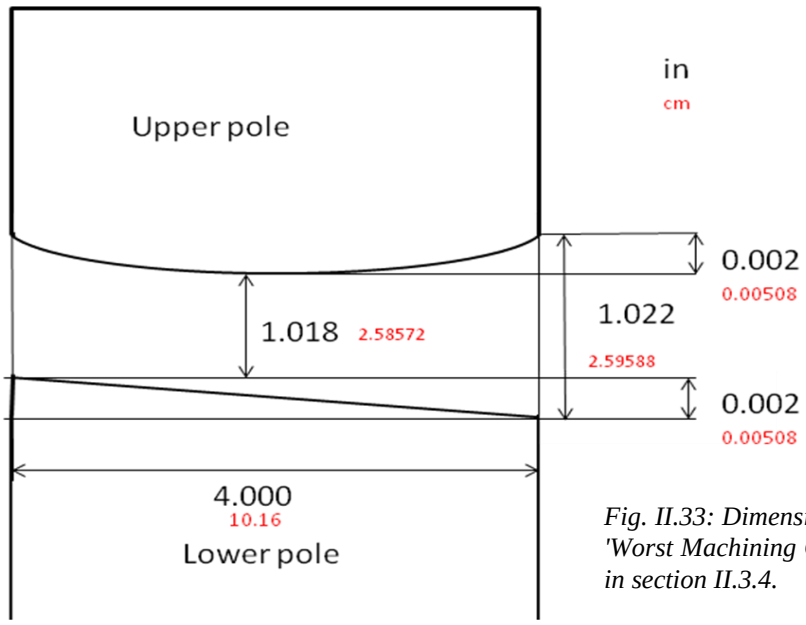

Equations of the slope and parabola:

$$y = \frac{0.00254}{5.08} \cdot x$$

$$y = 1.9685039370079 \cdot 10^{-4} \cdot x^2$$

Fig. II.33: Dimensional specifications of the 'Worst Machining Case that was introduced in section II.3.4.

Comparison of their field

Figure II.34 presents a plot of the skew quadrupole of the field induced by both the WMC and the $P = 50$ microns elliptic model. Several interesting points are to be noticed:

- the amounts of skew quadrupole induced by both models are very similar, which is quite reinsuring about the assumption that there could be a correlation between the amplitude of the geometric perturbation and the amplitude of defect in the field
- the quadrupole field induced by the $P = 50$ model has a slightly lower in absolute value, which is consistent with its having a slightly lower perturbation (50 microns versus 50.8 for the WMC model)
- the quadrupole fields induced by the two models have opposite signs. This is probably the effect of having a concave form instead of convex. Firstly, the purpose of this section is again to study quantitatively the influence of the perturbation amplitude, so a greater importance will be given to the amplitude of the field than to its sign. Of course and although it is very unlikely, if the latter were to change with the perturbation amplitude, this would be considered with great care. Secondly, we have seen that a concave shape is far more realistic than a convex one so the sign of the field induced by the elliptic model is more likely to have physical meaning.

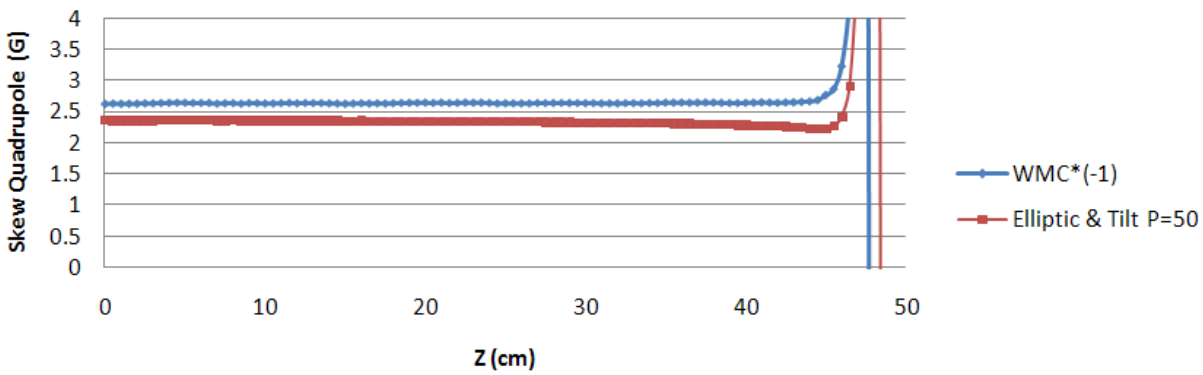

Fig. II.34: The skew quadrupole induced by the two compared models along the length of the dipole.

IV.3.2 - Multipoles behavior

After having calibrated the parameterized model, it was decided that it would be solved for different values of its parameter. Since the future magnets are a priori not expected to be designed with looser tolerances than the current magnets, the range for the variation of the parameter P was going to be 0 - 50 microns (Fig. II.35).

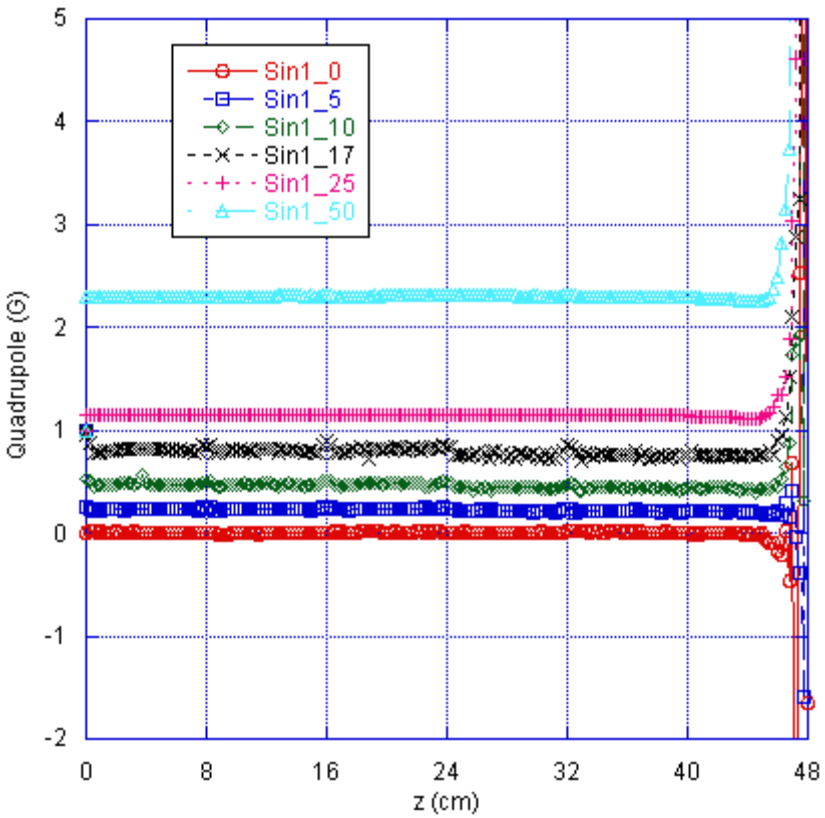

Fig. II.35: Skew quadrupole field induced by the perturbed models for P = 0, 5, 10, 17, 25 and 50 microns

One can observe that the value of the quadrupole field increases with the value of the geometrical perturbation which confirms a dependence. The next step is to determine the character of this dependence. To be able to plot the intensity of the field induced by the modeled magnets in function of their perturbation parameter, one needs a value that would represent the extent of the multipole content of the field for a given magnet. The integrated field along the beam path is widely used for that purpose. This integral:

$$\int_{beampath} \vec{B}.d\vec{l} \tag{7}$$

can be calculated for each multipole harmonic of the field independently, by linear property of the integral. In this case it is calculated numerically (with a finite step) using the table of evaluated fields generated by the script which evaluates the multipoles (II.3.5.2) [A3]. Each integral is however normalized by dividing the multipole value by

the normal dipole term (the principal field that bends the beam) so that one can see clearly the relative importance of a given term with respect to the ambient field. At first, the integrals will be computed over the portion of the beam path that corresponds to the gap between the poles (90 cm of the beam path, centered on the origin), for it was said that the study of the edges' contribution would come later.

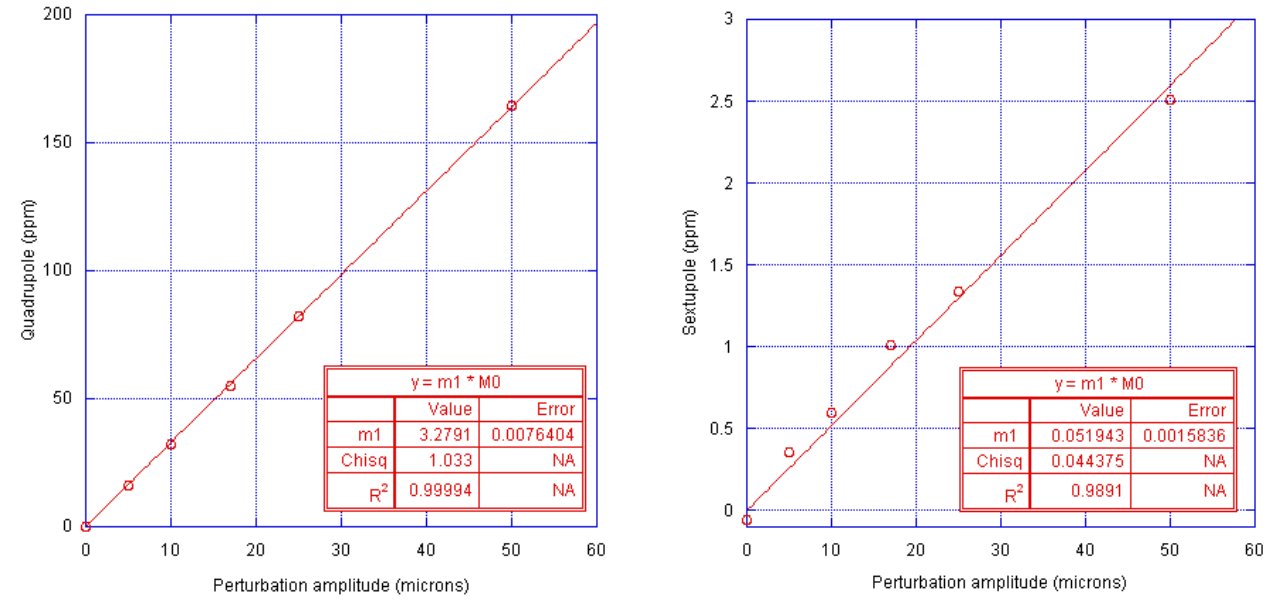

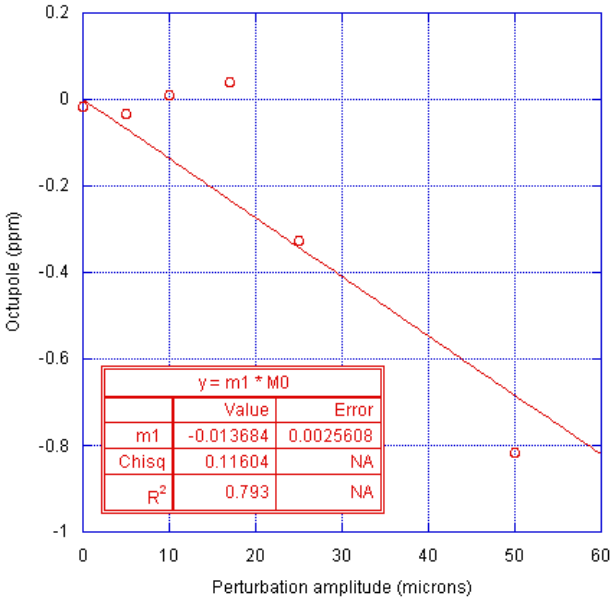

Fig. II.36: Skew quadrupole, sextupole and octupole terms integrated over the length of the body of the magnet. Units are parts per million of the normal dipole field. Linear fits have been associated with the plots.

Since this is a quantitative approach, higher order multipoles have been considered, to discover whether their content can be a significant perturbation for the particle beam.
The linear tendency seems established for the quadrupole term. It is not as clear for the sextupole and rather bold for the octupole term. It should however be noted that the values for the those fields are extremely low, and 1 ppm of a 14kG field that has been integrated over a ~100cm magnet only represents an ambient value of ~14mG/cm.
It has been established [7] that the finite element numerical code that is used to realize those calculations present a noise in its field values, mainly due to meshing issues, that

is around 50 mG in amplitude, that's to say around 4 ppm. That renders the graphs for sextupole and octupole terms not conclusive.

Since the variation of quadrupole and sextupole seem monotonic, a way of trying to determine a variation tendency for those terms anyway is to expand the range of variation of the geometrical parameter *P* so that a fit can be computed with higher values of the field, and then extrapolated to lower values of the geometrical perturbation (Fig. II.35).

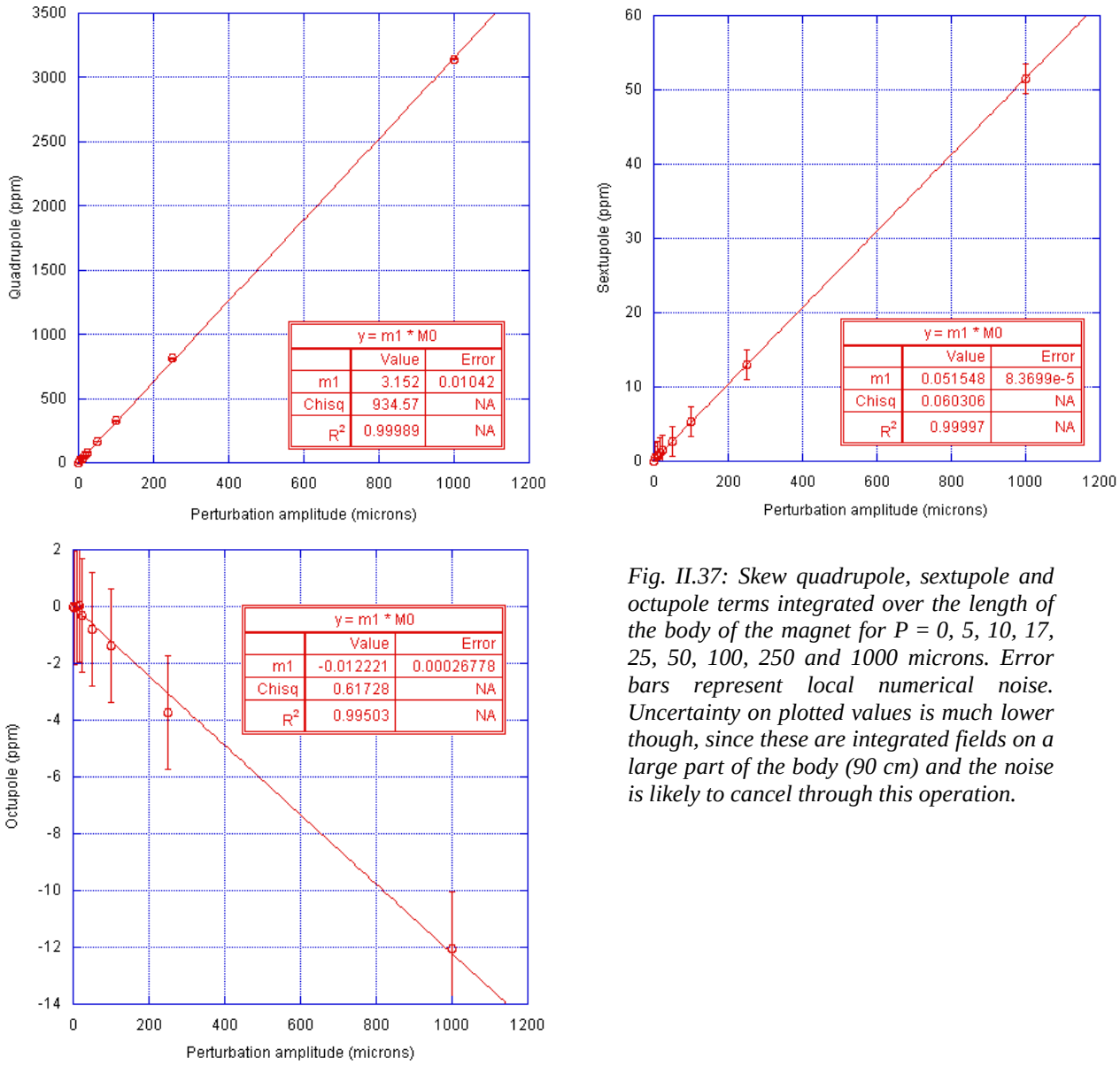

Fig. II.37: Skew quadrupole, sextupole and octupole terms integrated over the length of the body of the magnet for P = 0, 5, 10, 17, 25, 50, 100, 250 and 1000 microns. Error bars represent local numerical noise. Uncertainty on plotted values is much lower though, since these are integrated fields on a large part of the body (90 cm) and the noise is likely to cancel through this operation.

Given the accuracy of the fits, all three multipoles will be considered to have a linear dependence on the perturbation amplitude. Between figures II.36 and II.37, skew quadrupole and sextupole calculations are even consistent at the few percent level.
Now that the behavior of the field within the body is better understood, it shall be compared to the field that is seen near the edges of the poles, to ponder its relative

importance in the total integrated field seen by the beam as it travels through the whole magnet.

IV.3.3 - Relative importance of body and edge fields

Obtaining an accurate calculation of the field value near the edges of the poles is a difficult task on which Jefferson Lab scientists are still working. However, once refined the finite element mesh in that region, the values obtained were accurate enough to allow this study to go on and reach meaningful conclusions.

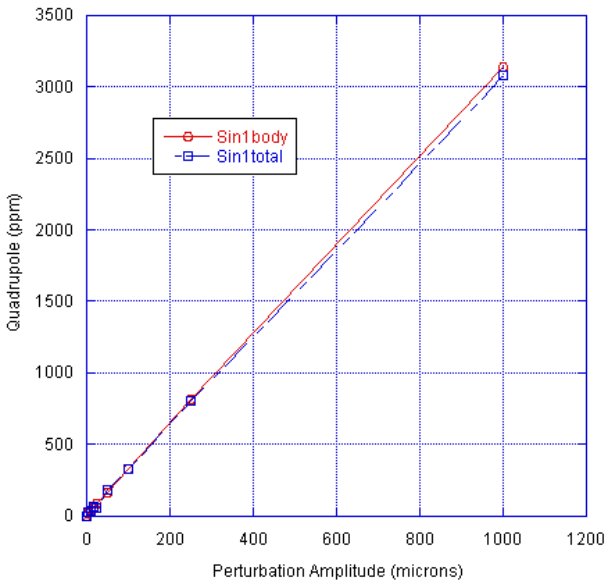

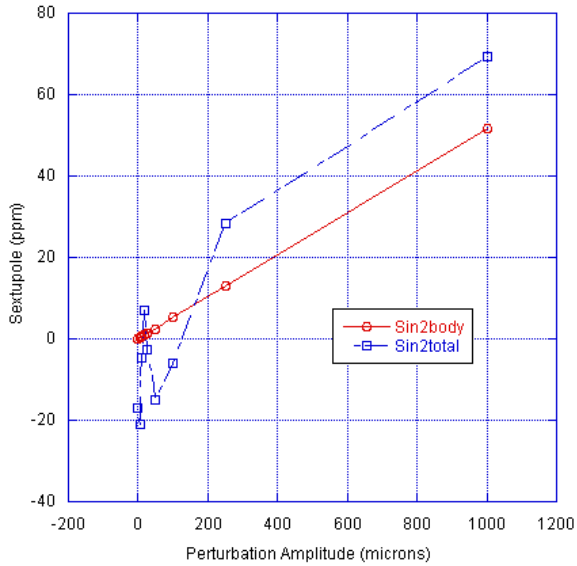

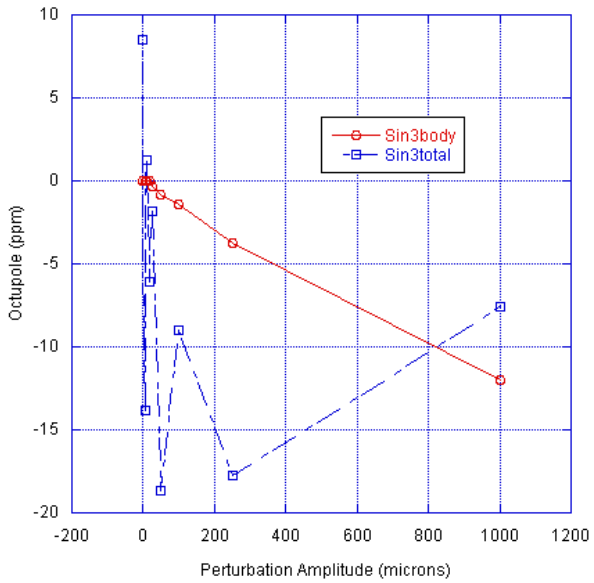

Fig. II.38: Comparison, for quadrupole, sextupole and octupole, of the integration over the inner part of the dipole (from z = -45 cm to z = 45 cm) with the integration over the whole length of the simulated trajectory (from z = -75 cm to z = 75 cm). The latter gets to zones where the field gets low enough to consider that the total influence of the magnet has been taken into account.

The quadrupole body term is obviously dominating the edges' field and imposes the tendency (fig. II.38). The integrated octupole over the whole model is very far from the body term. Its oscillations as the geometrical perturbation increases are very unlikely to have any physical meaning and this whole set of value is probably composed mainly of numerical noise.

The relation between the sextupole field integrated in the body and its integration over the whole model seems a bit stronger for high values of the perturbation, although the oscillation observable at low values clearly indicate that our uncertainty is too high to establish a relation.

Conclusions

The integrated field over the body has a linear behavior with respect to the amplitude of the geometrical perturbation of the pole tips for quadrupole, sextupole and octupole.
However, after comparison with the integrated fields over the total length of the considered beam trajectory, it appears that a clear dominance of the body term is only established for the quadrupole term, since the influence of numerical noise becomes too strong when it comes to the study of higher terms, which are much lower fields.

V - General conclusions

This section presents the final conclusions that the student's work, along with his supervisor's productive coaching led to.

1. The perturbation modeling technique is valid in the body of the magnet.
2. Skew quadrupole and sextupole calculated tendencies are consistent at the few percent level over a variation of a factor of 20 in their evaluation domain.
3. Skew terms at the end of the steel, where perturbations terminate, are more difficult to model. Ten variations of end mesh have been tried. One was found which did not increase the number of elements unduly and provided more physical results than those shown above. Unfortunately, time did not permit the work presented to be redone with the better mesh outside the steel. The results shown here which include the ends of the magnets are unfortunately not meaningful except to inform further development of magnet models.
4. However, since the geometrical perturbation only affects the steel, the integrated skew term outside of it should be close to zero, as it is in the non-perturbed models. Use only of the terms calculated in the body of the dipole is therefore reasonable.
5. Skew terms are ~20% larger in magnets in which the steel remains in the linear regime than in magnets approaching saturation.
6. Skew quadrupole predicted for 50 micron perturbation and 6 kG field (current specifications for the magnets) is two orders of magnitude higher than the ~1 G per meter of dipole seen in present CEBAF with beam. There cannot be a <u>systematic</u> machining or assembly error. Errors must be random and cancel in large part OR the vendor must have performed far better than specification, or both.
7. Skew sextupole at the level predicted would likely be seen in beam shape in the halls and isn't. Whether it is suppressed by one or two orders of magnitude for the same reasons as the skew quadrupole can't be determined by data available.
8. Skew terms in individual magnets immediately prior to a critical region, for instance the Compton polarimeter chicane dipoles, should be held to tight tolerance because there's no way to "average out" the random errors over short distances.
9. The 12 GeV project team must examine this work to determine whether they wish to tighten the tolerance on machining of new dipoles or to gamble that the vendor chosen will do as well as did the one who did the work in the early 1990's. Given the large cost to tighten tolerance on the sixty or so dipoles to be purchased, perhaps a modest incentive clause in the dipole contracts and dedicated skew correction elements in the hall transport lines are a good strategy.
10. Extreme care must be taken in disassembly and reassembly of the existing dipoles with H steel to ensure no systematic error is created.
11. Direct measurement of normal and skew terms through at least sextupole and perhaps decapole is desirable so magnets can be sorted to cancel skew terms locally.

VI - References, bibliography and annexes

VI.1 - References

Softwares

[1]: Opera Version 12.009 Professional Edition x64, Vector Fields Ltd, 24 Bankside, Kidlington, Oxford, OX5 1JE, UK, support@vectorfields.co.uk, http://www.vectorfields.com

[2]: Microsoft® Office Excel® 2007 (12.0.6214.1000) SP1 MSO (12.0.6213.1000), Part of Microsoft Office Professional Plus 2007, © 2006 Microsoft Corporation. All rights reserved.

[3]: Kaleidagraph *Tools for discovery*, Version 4.03, Copyright: 1986-2006 by Synergy Software

[8]: Océ, *Electronic Job Ticket for the Web*, http://dcg4/oceweb/Oce/Main/ASP/FS_Login.asp

Books

[4]: Foster, L. W., *Geo-metrics IIIm: the metric application of geometric dimensioning and tolerancing techniques, as based upon harmonization of national and international standard practices*, ISBN 0-201-63343-4, Addison-Wesley (1994)

Publications and technical notes

[5]: J.K.Cobb, R.S.Cole, *Spectroscopy of quadrupole magnets*, Proc. International Symposium on Magnet Technology (MT-1), Stanford, USA, (1965)

[6]: Y. Roblin and Arne Freyberger, *Studies of Beam Halo Formation in the 12 GeV CEBAF Design*, Jlab-TN-06-048 (2006)

[7]: J. Benesh, *Calculating Multipoles in Opera/TOSCA - mesh and software noise effects*, JLAB-TN-08-024 (2008)

VI.2 - Bibliography

The following material was used in a regular basis throughout this work and would be made reference to so often in this document that it was decided to list them as general references in this bibliography.

Presentations

Harwood, L., A. Lung and M. Wiseman, *12 GeV ACCELERATOR OVERVIEW*, Director's Project Review, Newport News (2005)

Books

The American Society of Mechanical Engineers, *Dimensioning and Tolerancing*, ANSI Y14.5M-1982

Wille, K., *The Physics of Particle Accelerators an introduction*, Oxford University Press (2000)

American Institute of Physics, *AIP CONFERENCE PROCEEDINGS 153 - PHYSICS OF PARTICLE ACCELERATORS, SLAC Summer School 1985, Fermilab Summer School 1984*, Melvin Month & Margaret Dienes (1987)

Internet

http://www.jlab.org/

http://www.wikipedia.org/

VI.3 - List of Annexes

[A1]	: An example of a post processor output file
[A2]	: The Perl script used to convert the post processor output file into a suitable format for spreadsheet exploitation
[A3]	: The script used to generate the circles along the beam path in the post processor
[A4]	: An example of a calculation report emitted by the code

Annex [A1]

```
Opera-3d Post-Processor Version 12.009   started on 25/May/2008 at 19:50:15
Copyright (c) 1984-2007, Vector Fields Limited, Oxford, UK.
Node: CASNRUIZ. Processor: EM64T/x64. System: Windows XP Professional x64 Edition
(Service Pack 2)
Command language initialisation.
Unit of Length           : CM
Unit of Magn Flux Den    : GAUSS
Unit of Magnetic Field   : OERSTED
Unit of Magn Scalar Pot  : OCM
Unit of Magn Vector Pot  : GCM
Unit of Conductivity     : SCM
Unit of Current density  : ACM2
Unit of Power            : WATT
Unit of Force            : NEWTON
Unit of Energy           : JOULE
Unit of Electric Field   : VCM
Unit of Elec Flux Den    : CCM2
Unit of Mass             : GRAMME
Information: opera.comi was not found in the local or home directory
*** CONTROL COMMAND ** $COMI
**** COMMAND INPUT ***
**** COMMAND INPUT *** ACTIVATE FILE='C:\Documents and Settings\nruiz\My
Documents\TOSCA\Spoiling\abh_jb14kG\extending models\2x100-
micron_elliptic_vs_tilt\2x100-micron_elliptic_vs_tilt_extended_minus8cm.op3'
Opening file for checking: C:\Documents and Settings\nruiz\My
Documents\TOSCA\Spoiling\abh_jb14kG\extending models\2x100-
micron_elliptic_vs_tilt\2x100-micron_elliptic_vs_tilt_extended_minus8cm.op3
**** COMMAND INPUT *** LOAD
Attaching file as resident: C:\Documents and Settings\nruiz\My
Documents\TOSCA\Spoiling\abh_jb14kG\extending models\2x100-
micron_elliptic_vs_tilt\2x100-micron_elliptic_vs_tilt_extended_minus8cm.op3
Opening database ...liptic_vs_tilt_extended_minus8cm.op3, simulation number 1 on
25/May/2008 at 19:50:20
TITLE=z=8cm cutting plane was removed
Unit of Length           : CM
Unit of Magn Flux Den    : GAUSS
Unit of Magnetic Field   : OERSTED
Unit of Magn Scalar Pot  : OCM
Unit of Magn Vector Pot  : GCM
Unit of Conductivity     : SCM
Unit of Current density  : ACM2
Unit of Power            : WATT
Unit of Force            : NEWTON
Unit of Energy           : JOULE
Unit of Electric Field   : VCM
Unit of Elec Flux Den    : CCM2
Unit of Mass             : GRAMME
**** COMMAND INPUT *** SELECT ACTION=DEFAULT
**** COMMAND INPUT *** SELECT ACTION=SELECT OPTION=SURFACES
**** COMMAND INPUT *** THREED OPTION=REFRESH
*** CONTROL COMMAND ** $COMI 'C:\Documents and Settings\nruiz\My
Documents\TOSCA\Comis\Dip_Eval_300_Nodal.comi' MODE=CONTINUOUS
Opening file for input: C:\Documents and Settings\nruiz\My
Documents\TOSCA\Comis\Dip_Eval_300_Nodal.comi
**** FILE INPUT ****** ACTIVATE CASE=1 MODELSYMMETRY=DATABASE
The resident file has been unloaded to allow the new file to be checked.
Opening file for checking: C:\Documents and Settings\nruiz\My
Documents\TOSCA\Spoiling\abh_jb14kG\extending models\2x100-
micron_elliptic_vs_tilt\2x100-micron_elliptic_vs_tilt_extended_minus8cm.op3
**** FILE INPUT ****** LOAD
Attaching file as resident: C:\Documents and Settings\nruiz\My
Documents\TOSCA\Spoiling\abh_jb14kG\extending models\2x100-
micron_elliptic_vs_tilt\2x100-micron_elliptic_vs_tilt_extended_minus8cm.op3
Opening database ...liptic_vs_tilt_extended_minus8cm.op3, simulation number 1 on
25/May/2008 at 19:50:53
TITLE=z=8cm cutting plane was removed
Unit of Length           : CM
Unit of Magn Flux Den    : GAUSS
Unit of Magnetic Field   : OERSTED
Unit of Magn Scalar Pot  : OCM
Unit of Magn Vector Pot  : GCM
Unit of Conductivity     : SCM
Unit of Current density  : ACM2
Unit of Power            : WATT
Unit of Force            : NEWTON
Unit of Energy           : JOULE
Unit of Electric Field   : VCM
Unit of Elec Flux Den    : CCM2
Unit of Mass             : GRAMME
**** FILE INPUT ****** SELECT ACTION=DEFAULT
**** FILE INPUT ****** SELECT ACTION=SELECT OPTION=SURFACES
**** FILE INPUT ******
**** FILE INPUT ****** THREED OPTION=GETVIEW
```

```
**** FILE INPUT ****** THREED OPTION=SETVIEW ROTX=-90 ROTY=0.01 ROTZ=0.01 SIZE=100
PERSPECTIVE=NO
**** FILE INPUT ****** SET FIELD=NODAL COIL=NODAL
**** FILE INPUT ****** set XLOCAL=0,YLOCAL=0,ZLOCAL=0,PLOCAL=0,TLOCAL=0,SLOCAL=0
**** FILE INPUT ****** CIRCLE RADIUS=1 TH1=0 TH2=360 ZC=0 NP=60
**** FILE INPUT ****** PLOT FILE=TEMP COMPONENT=By
X                 Y                 Z                 BY
1.0               0.0               0.0               -14163.221838764
0.99452189536827  0.10452846326765  0.0               -14162.806446465
0.97814760073381  0.20791169081776  0.0               -14162.510717193
0.95105651629515  0.30901699437495  0.0               -14162.341017265
0.9135454576426   0.4067366430758   0.0               -14162.25213583
0.86602540378444  0.5               0.0               -14162.210476839
0.80901699437495  0.58778525229247  0.0               -14162.165329251
0.74314482547739  0.66913060635886  0.0               -14162.067371641
0.66913060635886  0.74314482547739  0.0               -14161.914594433
0.58778525229247  0.80901699437495  0.0               -14161.662715689
0.5               0.86602540378444  0.0               -14161.333207984
0.4067366430758   0.9135454576426   0.0               -14160.916837241
0.30901699437495  0.95105651629515  0.0               -14160.441508285
0.20791169081776  0.97814760073381  0.0               -14159.914040818
0.10452846326765  0.99452189536827  0.0               -14159.369443517
0.0               1.0               0.0               -14158.822561159
-0.1045284632677  0.99452189536827  0.0               -14158.294760717
-0.2079116908178  0.97814760073381  0.0               -14157.783552069
-0.3090169943749  0.95105651629515  0.0               -14157.266117814
-0.4067366430758  0.9135454576426   0.0               -14156.74850479
-0.5              0.86602540378444  0.0               -14156.214193167
-0.5877852522925  0.80901699437495  0.0               -14155.658491549
-0.6691306063589  0.74314482547739  0.0               -14155.07654529
-0.7431448254774  0.66913060635886  0.0               -14154.482306533
-0.8090169943749  0.58778525229247  0.0               -14153.903318198
-0.8660254037844  0.5               0.0               -14153.369907659
-0.9135454576426  0.4067366430758   0.0               -14152.926629838
-0.9510565162952  0.30901699437495  0.0               -14152.618433451
-0.9781476007338  0.20791169081776  0.0               -14152.493506994
-0.9945218953683  0.10452846326765  0.0               -14152.589940569
-1.0              0.0               0.0               -14152.932915504
-0.9945218953683  -0.1045284632677  0.0               -14153.51801096
-0.9781476007338  -0.2079116908178  0.0               -14154.343419998
-0.9510565162952  -0.3090169943749  0.0               -14155.378395705
-0.9135454576426  -0.4067366430758  0.0               -14156.582637608
-0.8660254037844  -0.5              0.0               -14157.865888133
-0.8090169943749  -0.5877852522925  0.0               -14159.213505653
-0.7431448254774  -0.6691306063589  0.0               -14160.557094496
-0.6691306063589  -0.7431448254774  0.0               -14161.848552429
-0.5877852522925  -0.8090169943749  0.0               -14163.059517056
-0.5              -0.8660254037844  0.0               -14164.168265547
-0.4067366430758  -0.9135454576426  0.0               -14165.170902605
-0.3090169943749  -0.9510565162952  0.0               -14166.062913137
-0.2079116908178  -0.9781476007338  0.0               -14166.853519502
-0.1045284632677  -0.9945218953683  0.0               -14167.551863513
0.0               -1.0              0.0               -14168.162896764
0.10452846326765  -0.9945218953683  0.0               -14168.683218789
0.20791169081776  -0.9781476007338  0.0               -14169.099039803
0.30901699437495  -0.9510565162952  0.0               -14169.392133901
0.4067366430758   -0.9135454576426  0.0               -14169.536789695
0.5               -0.8660254037844  0.0               -14169.512690175
0.58778525229247  -0.8090169943749  0.0               -14169.312312022
0.66913060635886  -0.7431448254774  0.0               -14168.937056385
0.74314482547739  -0.6691306063589  0.0               -14168.400606992
0.80901699437495  -0.5877852522925  0.0               -14167.720236367
0.86602540378444  -0.5              0.0               -14166.925138756
0.9135454576426   -0.4067366430758  0.0               -14166.098348065
0.95105651629515  -0.3090169943749  0.0               -14165.265408849
0.97814760073381  -0.2079116908178  0.0               -14164.482016017
0.99452189536827  -0.1045284632677  0.0               -14163.783981529
1.0               0.0               0.0               -14163.221838764
Component: BY, from buffer: Circle
Minimum: -14169.5367896953, Maximum: -14152.4935069936
Integral = -88936.9800883494
**** FILE INPUT ****** FIT TYPE=FOURIER FILE=TEMP COMP=By ORDER=10 PRINT=YES
Polynomial fitting to tabulated values on a line
Component:  BY
Fourier coefficients
   Order       Sine term          Cosine term        Amplitude          Phase
   n            A_n                B_n
     0        0.0                -14161.229928783  14161.2299287827  179.999994991044
     1        4.65362551353294   -5.1715594743102  6.95710125099044  -138.01754624113
     2        0.06511040232441   2.71085332286577  2.7116351344868   -1.3758892829255
     3        -0.018629312841    0.02822737628213  0.03382064559852  33.4237420306027
     4        -6.226690931E-05   0.44176275077825  0.44176275516654  8.0758981544E-03
     5        -3.156967654E-03   -3.641395952E-03  4.8193577627E-03  139.075809756733
     6        1.463015892E-03    -1.04168556E-03   1.7959744724E-03  -125.45133672036
     7        8.1625057096E-04   4.8987181458E-06  8.1626527062E-04  -89.656141690398
     8        4.9866337026E-04   2.3009152433E-03  2.3543313517E-03  -12.228255562204
```

```
     9        1.3782763069E-04  -7.529855982E-04  7.654957654E-04   -169.62731411444
**** FILE INPUT ****** set xloc=1.374,0.000,74.981,2.699,0.000,0.000
**** FILE INPUT ****** circ
**** FILE INPUT ****** fit
Polynomial fitting to tabulated values on a line
Component:  BY
Fourier coefficients
   Order       Sine term         Cosine term       Amplitude         Phase
   n             A_n               B_n
     0        0.0               -5.4555288062005  5.45552880620054  179.999994991044
     1        -0.0168299773886  -0.1707010108206  0.17152866592515  174.369212576266
     2        5.0776727173E-03  0.03383178578031  0.03421070723193  -8.5355765642261
     3        0.01432123088062  -1.856113384E-03  0.01444101141992  -97.38469293707
     4        -6.691231953E-03  1.3234512454E-03  6.8208583218E-03  78.8119324375829
     5        -2.823309362E-03  -4.974628375E-03  5.719965316E-03   150.423275375887
     6        8.1448365678E-03  0.01101269519737  0.01369736537539  -36.486114453426
     7        6.191892909E-03   9.2542828953E-03  0.01113468857686  -33.785847576462
     8        -1.445175793E-03  9.037727344E-03   9.1525432868E-03  9.08495700215354
     9        -5.90514075E-03   1.6497468997E-03  6.1312602381E-03  74.3909795088685
**** FILE INPUT ****** set xloc=1.362,0.000,74.731,2.690,0.000,0.000
**** FILE INPUT ****** circ
**** FILE INPUT ****** fit
Polynomial fitting to tabulated values on a line
Component:  BY
Fourier coefficients
   Order       Sine term         Cosine term       Amplitude         Phase
   n             A_n               B_n
     0        0.0               -5.3960906761972  5.39609067619721  179.999994991044
     1        -6.303748054E-03  -0.1757395096984  0.17585253057193  177.945685371731
     2        -1.724816197E-03  0.04217618394546  0.04221143782336  2.34183463045649
     3        0.01593779981791  -6.554857298E-03  0.01723309656526  -112.35625622872
     4        2.8109563302E-03  7.1221023268E-03  7.6567497702E-03  -21.538192197483
     5        3.0424887929E-03  -2.715035426E-03  4.0777635316E-03  -131.74486353951
     6        -4.610919032E-03  6.9654883587E-03  8.3533587491E-03  33.5032184210446
     7        1.6607229841E-03  0.01022753106116  0.0103614860149   -9.2230589314923
     8        5.1316060632E-03  4.0134610763E-03  6.5146949736E-03  -51.970814350807
     9        5.1507520595E-03  -2.623088254E-03  5.7802109622E-03  -116.98806465358
**** FILE INPUT ****** set xloc=1.350,0.000,74.481,2.681,0.000,0.000
**** FILE INPUT ****** circ
**** FILE INPUT ****** fit
Polynomial fitting to tabulated values on a line
Component:  BY
Fourier coefficients
   Order       Sine term         Cosine term       Amplitude         Phase
   n             A_n               B_n
     0        0.0               -5.3226354037128  5.32263540371283  179.999994991044
     1        3.5975865751E-03  -0.1793324295713  0.1793685115206   -178.85073895747
     2        -3.540815259E-03  0.03329422539948  0.03348197750509  6.07054425273992
     3        8.0464508355E-03  6.8704450932E-03  0.01058056647002  -49.507711780297
     4        -0.0181358052348  -6.80834172E-03   0.01937165322033  110.576576514822
     5        -4.799463861E-03  -1.001028752E-03  4.9027453449E-03  101.781333762995
     6        -1.581774896E-03  -5.037607792E-03  5.2801045529E-03  162.56805835838
     7        -6.340173195E-04  0.01622444987614  0.01623683318092  2.23785962239485
     8        -2.00519836E-03   5.8541896055E-03  6.1880818029E-03  18.907544000601
     9        3.3446749663E-03  -7.721660831E-04  3.4326507382E-03  -102.99978609285
**** FILE INPUT ****** set xloc=1.338,0.000,74.232,2.672,0.000,0.000
**** FILE INPUT ****** circ
**** FILE INPUT ****** fit
Polynomial fitting to tabulated values on a line
Component:  BY
Fourier coefficients
   Order       Sine term         Cosine term       Amplitude         Phase
   n             A_n               B_n
     0        0.0               -5.2365498124121  5.2365498124121   179.999994991044
     1        9.6710022669E-03  -0.1630760471865  0.16336255828933  -176.60612206643
     2        0.01765975976018  0.01972255920183  0.02647350479738  -41.841554870655
     3        -9.447436244E-03  6.0596624357E-03  0.01122379438613  57.3235558030462
     4        -5.783492371E-03  -0.0179566940429  0.01886509064256  162.147282956251
     5        -6.828364476E-03  3.3041885457E-03  7.585790886E-03   64.1780461042141
     6        8.9752446137E-03  -2.053754204E-03  9.207221199E-03   -102.88876787707
     7        -3.182523228E-03  0.01109710489124  0.01154444416432  16.0022876545783
     8        -8.947663227E-03  3.0604180317E-04  8.9528955543E-03  88.041042446106
     9        2.9118555872E-03  0.01248614979323  0.0128211871377   -13.127148647153
**** FILE INPUT ****** set xloc=1.327,0.000,73.982,2.663,0.000,0.000
**** FILE INPUT ****** circ
**** FILE INPUT ****** fit
Polynomial fitting to tabulated values on a line
Component:  BY
Fourier coefficients
   Order       Sine term         Cosine term       Amplitude         Phase
   n             A_n               B_n
     0        0.0               -5.1399744669276  5.13997446692761  179.999994991044
     1        0.01784765672023  -0.1611717519349  0.16215693778607  -173.68098474899
     2        0.01308234533318  0.0217545679869   0.02538521198874  -31.021052524404
     3        -1.263289006E-03  5.9076636117E-03  6.0412240864E-03  12.0702845141411
     4        4.8439101676E-03  -6.797978796E-03  8.3472139919E-03  -144.5281656903
```

```
     5        7.6228602747E-04  -4.313425215E-03  4.3802644979E-03  -169.97793168579
     6        7.0224167183E-03  5.7685872572E-03  9.0879555187E-03  -50.598492566929
     7        -4.831385993E-04  0.01411432841265  0.0141225949969   1.9604898598809
     8        -6.320537285E-04  6.1656790677E-03  6.1979908262E-03  5.85303748566267
     9        -3.348580958E-03  8.9390734754E-03  9.5456811717E-03  20.5359719157808
**** FILE INPUT ****** set xloc=1.315,0.000,73.732,2.654,0.000,0.000
**** FILE INPUT ****** circ
**** FILE INPUT ****** fit
Polynomial fitting to tabulated values on a line
Component:  BY
Fourier coefficients
   Order       Sine term         Cosine term       Amplitude         Phase
   n             A_n               B_n
     0        0.0               -5.0447333605769  5.04473336057689  179.999994991044
     1        0.02123581632123  -0.1526867354578  0.15415641108815  -172.08203671952
     2        4.1953513972E-03  1.8289375564E-04  4.1993360752E-03  -87.503803921773
     3        -0.0160653871389  -0.0130001118032  0.02066638746413  128.979781825153
     4        3.422772327E-03   6.7299790728E-03  7.5503634828E-03  -26.957245081729
     5        6.0712280479E-03  -2.878639534E-03  6.7191052661E-03  -115.36770967612
     6        9.887445942E-03   -3.192005559E-03  0.0103899223647   -107.89185025874
     7        -3.013360418E-03  0.01294211458046  0.01328829074108  13.1068701351751
     8        9.0359476595E-03  2.4155459052E-03  9.3532460742E-03  -75.033304737512
     9        -5.831596302E-03  9.9000123276E-03  0.0114898981509   30.5001855306647
**** FILE INPUT ****** set xloc=1.304,0.000,73.482,2.645,0.000,0.000
**** FILE INPUT ****** circ
**** FILE INPUT ****** fit
Polynomial fitting to tabulated values on a line
Component:  BY
Fourier coefficients
   Order       Sine term         Cosine term       Amplitude         Phase
   n             A_n               B_n
     0        0.0               -4.9478856805132  4.94788568051322  179.999994991044
     1        0.01050345038872  -0.1604141346341  0.16075763453248  -176.25378184841
     2        -0.0140916820987  0.01032898438486  0.01747178934151  53.7591605019161
     3        -3.685393007E-03  -8.486052151E-03  9.2517675457E-03  156.525254286864
     4        6.4949583244E-04  9.1377633271E-03  9.1608167462E-03  -4.0656436625791
     5        3.9731102382E-03  -0.0125276007275  0.01314254103862  -162.40364732435
     6        2.775600168E-04   4.5848136044E-03  4.593207523E-03   -3.4644007444617
     7        -9.681876291E-03  -2.748728041E-03  0.01006450368206  105.849478872961
     8        3.78303312E-03    0.01401998437927  0.01452140838838  -15.100574838281
     9        -1.42780682E-03   0.01130736659921  0.01139715629987  7.19677896128044
**** FILE INPUT ****** set xloc=1.292,0.000,73.232,2.636,0.000,0.000
**** FILE INPUT ****** circ
**** FILE INPUT ****** fit
Polynomial fitting to tabulated values on a line
Component:  BY
Fourier coefficients
   Order       Sine term         Cosine term       Amplitude         Phase
   n             A_n               B_n
     0        0.0               -4.8401295503025  4.84012955030248  179.999994991044
     1        8.9290400378E-03  -0.164845536941   0.16508718546682  -176.89953593107
     2        -0.0150331387836  -7.39200321E-04   0.01505130156502  92.8150432003212
     3        -9.466765608E-03  -0.0126126271511  0.01577016216573  143.108894442669
     4        -4.12096114E-03   6.2448534677E-03  7.482012801E-03   33.4207061061371
     5        -0.0126769018456  -0.0290687968947  0.03171275442634  156.437980548225
     6        7.9278630479E-03  8.1819275815E-03  0.0113927587289   -44.096472516201
     7        -8.062370716E-03  -6.563520868E-03  0.01039623142075  129.148796086931
     8        0.01070028932416  0.01043341965579  0.01494498033905  -45.72347291939
     9        -6.382300157E-03  5.6676717275E-05  6.3825518048E-03  89.4912073776728
**** FILE INPUT ****** set xloc=1.281,0.000,72.983,2.627,0.000,0.000
**** FILE INPUT ****** circ
**** FILE INPUT ****** fit
Polynomial fitting to tabulated values on a line
Component:  BY
Fourier coefficients
   Order       Sine term         Cosine term       Amplitude         Phase
   n             A_n               B_n
     0        0.0               -4.7256698636916  4.72566986369159  179.999994991044
     1        0.0103644251464   -0.1719950980788  0.1723070952449   -176.55152131145
     2        -6.198996998E-03  -4.612937322E-03  7.7270145928E-03  126.654500287176
     3        -0.0200267375188  5.1584525719E-03  0.0206804218667   75.5558267270421
     4        -4.546729998E-03  -2.961238211E-03  5.4260192971E-03  123.075778533519
     5        7.3149632177E-04  -0.0224369588587  0.02244887992071  -178.13268262058
     6        -0.0104595995942  1.4424625171E-03  0.01055859468798  82.1479792522418
     7        -8.089557457E-03  3.1051841128E-03  8.6650509646E-03  69.0006527627503
     8        8.1664482581E-03  -1.804387129E-03  8.3634137805E-03  -102.45939294564
     9        -5.518281661E-04  -4.189042044E-03  4.2252322506E-03  172.495554273329
**** FILE INPUT ****** set xloc=1.269,0.000,72.733,2.618,0.000,0.000
**** FILE INPUT ****** circ
**** FILE INPUT ****** fit
Polynomial fitting to tabulated values on a line
Component:  BY
Fourier coefficients
   Order       Sine term         Cosine term       Amplitude         Phase
   n             A_n               B_n
     0        0.0               -4.6233375157648  4.62333751576476  179.999994991044
```

```
     1        0.0219927667348   -0.1837783390834  0.18508959912679  -173.17585773406
     2        -2.581049507E-03  -0.0147597499746  0.0149837257005   170.080931732679
     3        -0.0178124855031  9.8648630972E-03  0.0203617328271   61.0215545940324
     4        -0.0213738261309  -9.758817403E-03  0.02349627546201  114.540389721903
     5        0.01377321290566  -1.247675632E-03  0.01382960911331  -95.176129122927
     6        -1.459649679E-03  -0.012983218081   0.01306501163123  173.585402329276
     7        -7.281407948E-03  -3.991718258E-03  8.3037772346E-03  118.731854980857
     8        1.6930444232E-03  -3.298373776E-03  3.7075152035E-03  -152.82871514724
     9        0.01945241172045  -5.741288033E-03  0.02028197993353  -106.44371492917
**** FILE INPUT ****** set xloc=1.258,0.000,72.483,2.609,0.000,0.000
**** FILE INPUT ****** circ
**** FILE INPUT ****** fit
Polynomial fitting to tabulated values on a line
Component:  BY
Fourier coefficients
   Order       Sine term         Cosine term       Amplitude         Phase
   n             A_n               B_n
     0        0.0               -4.5005921992228  4.50059219922278  179.999994991044
     1        0.02243467518584  -0.180034604897   0.18142704762828  -172.89680501802
     2        5.2984666972E-03  -0.0147610095509  0.01568314867314  -160.25438731864
     3        -0.0183075303818  -3.298442573E-03  0.01860229534456  100.213328939248
     4        -0.0199270464637  -0.0277422731559  0.03415729644783  144.31061987589
     5        0.01173882328007  3.6262131214E-04  0.01174442277069  -88.230649340856
     6        1.285607817E-03   -0.0226197465026  0.02265625121906  -176.74705229987
     7        -6.213143399E-03  -2.855661608E-03  6.837978803E-03   114.68427663074
     8        -3.976529788E-03  -0.0131604385863  0.01374808833749  163.187391614213
     9        1.9868299109E-03  1.7160682256E-03  2.6253348834E-03  -49.182112372073
**** FILE INPUT ****** set xloc=1.246,0.000,72.233,2.600,0.000,0.000
**** FILE INPUT ****** circ
**** FILE INPUT ****** fit
Polynomial fitting to tabulated values on a line
Component:  BY
Fourier coefficients
   Order       Sine term         Cosine term       Amplitude         Phase
   n             A_n               B_n
     0        0.0               -4.3644466324416  4.36444663244158  179.999994991044
     1        0.02332330005347  -0.1729240278609  0.17448981556816  -172.31852542825
     2        9.2438590244E-03  -0.0126348791979  0.01565532184305  -143.81025778957
     3        -1.873216912E-03  -1.866459026E-03  2.6443545329E-03  134.896458416811
     4        -0.0192091270998  -0.0382454949587  0.04279846315665  153.331513495255
     5        0.01498818203654  1.0703062619E-03  0.0150263487333   -85.915438799075
     6        -0.0127514724869  -0.0419697613491  0.04386411880207  163.099890437751
     7        0.01162286111938  -0.0113507226872  0.01624591659843  -134.32131876523
     8        -9.478348447E-03  5.759649181E-04   9.4958319736E-03  86.5226164461483
     9        -6.84564669E-03   1.9479293266E-03  7.1173946964E-03  74.1162906848878
**** FILE INPUT ****** set xloc=1.235,0.000,71.984,2.591,0.000,0.000
**** FILE INPUT ****** circ
**** FILE INPUT ****** fit
Polynomial fitting to tabulated values on a line
Component:  BY
Fourier coefficients
   Order       Sine term         Cosine term       Amplitude         Phase
   n             A_n               B_n
     0        0.0               -4.2497924492698  4.2497924492698   179.999994991044
     1        0.01278048625356  -0.1864177300278  0.18685532076336  -176.07802980255
     2        -0.024654278111   0.02814582883659  0.0374168559619   41.2166678101678
     3        0.01341738686851  2.7828163464E-03  0.0137029317008   -78.282764051757
     4        -0.0181170493595  -0.0100635464954  0.020724440778    119.051021776109
     5        7.8901662887E-03  4.3430835541E-03  9.0065031406E-03  -61.169739139982
     6        -0.0269781552644  -4.119739513E-03  0.02729089802712  98.6823607061154
     7        9.3766193909E-03  -0.0153852218786  0.01801738170364  -148.63951671479
     8        0.01264267600445  -6.945726336E-03  0.01442499119205  -118.78383379546
     9        6.5057957104E-03  1.9653220975E-04  6.5087635335E-03  -88.269687646523
**** FILE INPUT ****** set xloc=1.224,0.000,71.734,2.582,0.000,0.000
**** FILE INPUT ****** circ
**** FILE INPUT ****** fit
Polynomial fitting to tabulated values on a line
Component:  BY
Fourier coefficients
   Order       Sine term         Cosine term       Amplitude         Phase
   n             A_n               B_n
     0        0.0               -4.1051794781058  4.10517947810584  179.999994991044
     1        -6.115662756E-03  -0.1801752178958  0.18027897956985  178.055958601917
     2        -0.0389153307612  9.720159284E-03   0.04011090206868  75.975773890947
     3        1.4082093542E-03  0.02232540957081  0.02236977796245  -3.6092372620495
     4        -0.0179579684649  0.01096367091403  0.02104021652215  58.5951633764696
     5        -1.366461955E-03  0.02355019550527  0.02358980556536  3.32077137014595
     6        4.0295633064E-03  0.019958819678    0.02036152900397  -11.414231214432
     7        2.3216657447E-03  -1.02433911E-03   2.5375977698E-03  -113.80748576549
     8        4.4739221979E-04  3.8685756914E-03  3.8943597263E-03  -6.5968245676143
     9        8.6234316793E-03  4.3274088292E-04  8.6342827495E-03  -87.12719171419
**** FILE INPUT ****** set xloc=1.213,0.000,71.484,2.573,0.000,0.000
**** FILE INPUT ****** circ
**** FILE INPUT ****** fit
Polynomial fitting to tabulated values on a line
Component:  BY
```

```
Fourier coefficients
   Order       Sine term         Cosine term       Amplitude         Phase
   n             A_n               B_n
     0        0.0               -3.9423143112273  3.94231431122734  179.999994991044
     1        1.1001155694E-03  -0.1737131538566  0.17371663730653  -179.63714892377
     2        -0.0175869721928  7.969056105E-04   0.01760501773531  87.4055704644047
     3        -0.0126037664606  9.781224356E-03   0.01595391108457  52.1865451127314
     4        -3.151805431E-03  0.01115816064694  0.01159475857857  15.7732024650905
     5        -2.22073355E-03   8.0672348484E-03  8.3673135233E-03  15.3910665307226
     6        0.0142643794998   -1.193819784E-03  0.01431424913126  -94.784068089167
     7        -8.805528549E-03  -8.040709259E-04  8.8421639361E-03  95.2174535005397
     8        -0.0133916704794  -3.872211833E-03  0.01394026049633  106.127263218246
     9        -2.433923257E-03  -7.020755753E-03  7.4306792259E-03  160.879822875449
**** FILE INPUT ****** set xloc=1.201,0.000,71.234,2.564,0.000,0.000
**** FILE INPUT ****** circ
**** FILE INPUT ****** fit
Polynomial fitting to tabulated values on a line
Component:  BY
Fourier coefficients
   Order       Sine term         Cosine term       Amplitude         Phase
   n             A_n               B_n
     0        0.0               -3.7814111632706  3.78141116327056  179.999994991044
     1        8.1509087264E-03  -0.1900788496673  0.19025353190917  -177.54455758571
     2        0.01695483801069  -0.0100733520207  0.01972153525722  -120.71574927529
     3        -0.0262924768067  2.7118900243E-03  0.02643196330461  84.1111519321674
     4        0.01072770693989  1.2448113038E-03  0.01079968755891  -83.381166025254
     5        1.7758531526E-03  -4.275854915E-03  4.6299664873E-03  -157.44584829101
     6        0.01455836544061  -0.0169165809629  0.02231852853072  -139.28479511806
     7        -1.474641101E-03  -0.0122102870099  0.0122990111489   173.113712348495
     8        4.3157423451E-03  5.8183169669E-03  7.2442007369E-03  -36.566211439185
     9        -2.806533209E-03  -0.0164959014511  0.01673294335556  170.344422261072
**** FILE INPUT ****** set xloc=1.190,0.000,70.985,2.555,0.000,0.000
**** FILE INPUT ****** circ
**** FILE INPUT ****** fit
Polynomial fitting to tabulated values on a line
Component:  BY
Fourier coefficients
   Order       Sine term         Cosine term       Amplitude         Phase
   n             A_n               B_n
     0        0.0               -3.6557890419703  3.65578904197028  179.999994991044
     1        9.4086848809E-03  -0.189368306612   0.18960189582459  -177.15561726328
     2        0.01573703177383  -0.0125652628203  0.02013802370626  -128.60567847531
     3        -0.0104008589286  -0.0145011131213  0.01784545175139  144.350181633111
     4        5.0414200392E-03  3.9538449793E-03  6.4069342226E-03  -51.893899047621
     5        0.01347977084369  -5.936967453E-03  0.01472928391123  -113.77038537408
     6        -0.0130196940196  -0.0137663111658  0.0189479221942   136.596611214775
     7        -8.534104531E-03  -9.51401277E-03   0.01278074251079  138.107773770795
     8        2.2154564125E-03  -0.0101159624378  0.01035572031096  -167.64691121537
     9        5.8455455992E-03  -9.123273069E-04  5.9163117284E-03  -98.870713111373
**** FILE INPUT ****** set xloc=1.179,0.000,70.735,2.546,0.000,0.000
**** FILE INPUT ****** circ
**** FILE INPUT ****** fit
Polynomial fitting to tabulated values on a line
Component:  BY
Fourier coefficients
   Order       Sine term         Cosine term       Amplitude         Phase
   n             A_n               B_n
     0        0.0               -3.4951991519081  3.49519915190815  179.999994991044
     1        -0.0164025012607  -0.1779722672294  0.17872652279498  174.734305716263
     2        3.8519185985E-03  9.6521322079E-03  0.01039234973661  -21.75567482537
     3        -3.37024042E-03   0.0105843241364   0.01110794481061  17.662416454959
     4        3.7299243687E-03  5.1973648317E-03  6.3972601158E-03  -35.665370069252
     5        0.01105203040909  3.5256122496E-03  0.01160074643708  -72.307246656238
     6        -0.0225954090602  7.4623691127E-03  0.02379578667265  71.7236538546793
     7        -2.350890087E-03  -0.0126258814136  0.01284287996011  169.452526820164
     8        -0.010813291612   -6.64160277E-03   0.01269008127776  121.558546895691
     9        5.9394803992E-03  2.1628634465E-03  6.3210288483E-03  -69.99088947862
**** FILE INPUT ****** set xloc=1.168,0.000,70.485,2.537,0.000,0.000
**** FILE INPUT ****** circ
**** FILE INPUT ****** fit
Polynomial fitting to tabulated values on a line
Component:  BY
Fourier coefficients
   Order       Sine term         Cosine term       Amplitude         Phase
   n             A_n               B_n
     0        0.0               -3.3383440052784  3.33834400527838  179.999994991044
     1        -0.016652837716   -0.1693721247774  0.17018881765737  174.384664553673
     2        -0.0135099630128  0.01068602641471  0.01722527971163  51.6569260388887
     3        3.7455166458E-03  -3.413603167E-03  5.0676998261E-03  -132.34553125859
     4        5.4674784524E-03  0.0203582419118   0.02107964265274  -15.03282809465
     5        4.4634628352E-03  5.8157895471E-03  7.3311601086E-03  -37.505272725832
     6        -0.0190774103469  0.0114991173963   0.02227503729372  58.9200680400118
     7        -3.551419199E-03  -5.203454444E-03  6.2998822588E-03  145.685997149324
     8        -5.45530537E-03   -3.649007139E-04  5.4674956986E-03  93.8267627231636
     9        1.7540300152E-03  -1.676077308E-03  2.4260784067E-03  -133.69811501093
**** FILE INPUT ****** set xloc=1.157,0.000,70.235,2.528,0.000,0.000
```

```
**** FILE INPUT ****** circ
**** FILE INPUT ****** fit
Polynomial fitting to tabulated values on a line
Component:  BY
Fourier coefficients
   Order       Sine term         Cosine term       Amplitude         Phase
   n             A_n               B_n
     0        0.0               -3.1911659157589  3.19116591575893  179.999994991044
     1        -0.0213468235941  -0.1669597762552  0.16831890495349  172.713911749918
     2        0.0224712750533   0.01408915244608  0.02652286596825  -57.912903132965
     3        2.7365690604E-03  0.011482396847    0.01180399286574  -13.405081570797
     4        -0.0118088708573  0.02155876927841  0.02458108955526  28.7118358882224
     5        2.501954905E-03   -0.0210381377514  0.021186387573    -173.2179631931
     6        -7.96154794E-03   -0.0242003576502  0.02547633325251  161.789579805326
     7        -3.027153992E-03  -3.573963156E-03  4.683681664E-03   139.735329648015
     8        -5.384823206E-03  0.01442465187653  0.01539697706445  20.4709536303389
     9        4.043831777E-03   0.01541563923087  0.01593720516079  -14.698659158985
**** FILE INPUT ****** set xloc=1.146,0.000,69.985,2.519,0.000,0.000
**** FILE INPUT ****** circ
**** FILE INPUT ****** fit
Polynomial fitting to tabulated values on a line
Component:  BY
Fourier coefficients
   Order       Sine term         Cosine term       Amplitude         Phase
   n             A_n               B_n
     0        0.0               -3.0174192416997  3.01741924169968  179.999994991044
     1        -0.0204480544002  -0.1862703178231  0.18738931194349  173.735364430794
     2        0.01553552205603  0.02057449980678  0.02578104900605  -37.055951215887
     3        0.01741989191843  8.4726921027E-04  0.01744048449913  -87.215438169163
     4        -0.0405866477116  -0.0178369244481  0.04433319124797  113.724412267208
     5        8.0767787703E-03  -0.0305241431861  0.03157463653869  -165.17902621608
     6        -9.085737112E-03  -0.0306896450538  0.03200632644337  163.508491575768
     7        2.4090745182E-04  0.0109425339535   0.01094518550432  -1.2612024332862
     8        -0.0148532399295  0.01534251911048  0.02135442879263  44.0716836761603
     9        2.3585167472E-03  0.02604938610492  0.02615593847847  -5.1734656806376

                                        ...

Since the original output file was 90 pages long, this version only presents the data
for the first 5 cm and the last 5 cm of the 75cm-long evaluation path.

                                        ...

**** FILE INPUT ****** set xloc=-0.385,0.000,5.001,0.180,0.000,0.000
**** FILE INPUT ****** circ
**** FILE INPUT ****** fit
Polynomial fitting to tabulated values on a line
Component:  BY
Fourier coefficients
   Order       Sine term         Cosine term       Amplitude         Phase
   n             A_n               B_n
     0        0.0               -14156.041317707  14156.0413177069  179.999994991044
     1        4.5951485400029   -7.3097404663453  8.63410075167168  -147.84514705819
     2        0.08826948971471  3.07454575598527  3.07581259319574  -1.6444966596693
     3        -0.0246109877334  -0.6537103023218  0.65417341743522  177.843932851192
     4        8.6387642104E-03  0.4518880836371   0.45197064991025  -1.0951924824021
     5        -5.428728242E-03  -0.0174350781698  0.01826069662176  162.705069873042
     6        4.6597787634E-04  0.01573347049933  0.01574036941544  -1.6964319900966
     7        2.6026486319E-04  -0.0115532894605  0.01155622062604  -178.70949187604
     8        -6.013034293E-04  3.1274977119E-03  3.1847775043E-03  10.8830809884736
     9        -3.800017731E-04  5.8726407403E-04  6.994858399E-04   32.9057490005029
**** FILE INPUT ****** set xloc=-0.385,0.000,4.751,0.171,0.000,0.000
**** FILE INPUT ****** circ
**** FILE INPUT ****** fit
Polynomial fitting to tabulated values on a line
Component:  BY
Fourier coefficients
   Order       Sine term         Cosine term       Amplitude         Phase
   n             A_n               B_n
     0        0.0               -14156.316516893  14156.3165168925  179.999994991044
     1        4.59427198888759  -7.3098063742938  8.63369007652829  -147.85030463473
     2        0.0887373594782   3.07317479514165  3.07445566571728  -1.6539455362654
     3        -0.0255371689065  -0.6540844556887  0.65458278480984  177.764153465522
     4        9.1665665751E-03  0.45155765610684  0.45165068662793  -1.1629377342025
     5        -5.591234295E-03  -0.0179099130136  0.01876237951589  162.662332857737
     6        5.7978402152E-04  0.01780932784834  0.01781876280557  -1.8646098653777
     7        1.1790101609E-03  -0.0123069722811  0.01236331798862  -174.52774920304
     8        -2.619115258E-05  3.4676737213E-03  3.46777263E-03    0.43274369142114
     9        1.1080257832E-03  5.1225259193E-04  1.2207062932E-03  -65.188374618286
**** FILE INPUT ****** set xloc=-0.386,0.000,4.501,0.162,0.000,0.000
**** FILE INPUT ****** circ
**** FILE INPUT ****** fit
Polynomial fitting to tabulated values on a line
Component:  BY
Fourier coefficients
   Order       Sine term         Cosine term       Amplitude         Phase
```

```
   n            A_n                B_n
     0        0.0                -14156.568206666  14156.5682066664  179.999994991044
     1        4.59524879477979   -7.3167174291913  8.64006165629374  -147.86920797982
     2        0.08861482685431   3.07865282837395  3.07992789285615  -1.6487256778701
     3        -0.0252585491024   -0.6573739831733  0.65785906397642  177.799578351724
     4        9.2669440085E-03   0.45250199889881  0.45259687941774  -1.1732159360174
     5        -6.66074035E-03    -0.0167486082263  0.01802446502735  158.312814880565
     6        3.7866494438E-04   0.0156231907003   0.01562777894641  -1.3884267339699
     7        3.6361800472E-04   -0.0112738241858  0.01127968660142  -178.15265762608
     8        -5.938749438E-05   2.167359264E-03   2.1681727454E-03  1.56956050195495
     9        8.9195422295E-04   -5.385171848E-04  1.0419131894E-03  -121.12146816221
**** FILE INPUT ****** set xloc=-0.387,0.000,4.250,0.153,0.000,0.000
**** FILE INPUT ****** circ
**** FILE INPUT ****** fit
Polynomial fitting to tabulated values on a line
Component:  BY
Fourier coefficients
   Order       Sine term          Cosine term       Amplitude          Phase
   n            A_n                B_n
     0        0.0                -14156.809536304  14156.8095363039  179.999994991044
     1        4.59580924557914   -7.3198122079814  8.64298058437387  -147.87697311984
     2        0.09062567627986   3.07882876040227  3.08016226018718  -1.6860209433793
     3        -0.0250227112021   -0.659663417032   0.66013783397581  177.827661915806
     4        0.01036629086909   0.45391340593383  0.45403176108378  -1.308270400441
     5        -3.756424636E-03   -0.0190566095737  0.01942331316973  168.848856803027
     6        9.7488853613E-04   0.01850433953311  0.0185300024073   -3.015800875532
     7        6.4872970064E-04   -0.0138413415329  0.01385653584615  -177.31656348769
     8        3.5853526084E-04   4.9311533615E-03  4.9441704065E-03  -4.1585548619044
     9        9.5133143078E-04   -8.613100132E-04  1.2833107301E-03  -132.15684546337
**** FILE INPUT ****** set xloc=-0.388,0.000,4.000,0.144,0.000,0.000
**** FILE INPUT ****** circ
**** FILE INPUT ****** fit
Polynomial fitting to tabulated values on a line
Component:  BY
Fourier coefficients
   Order       Sine term          Cosine term       Amplitude          Phase
   n            A_n                B_n
     0        0.0                -14157.0334308    14157.0334308004  179.999994991044
     1        4.59242866874457   -7.3260645746097  8.64648039544755  -147.9179755991
     2        0.09104169946606   3.08130036699055  3.08264505622327  -1.6923984124558
     3        -0.0277250848964   -0.6633078177722  0.66388699448799  177.606526784221
     4        8.7810788459E-03   0.45351201906055  0.45359702245284  -1.1092448776924
     5        -5.167656277E-03   -0.0170964024314  0.01786033727263  163.181728541198
     6        1.088014521E-03    0.01883459219835  0.01886599159535  -3.3061207143177
     7        -1.476576758E-03   -0.0131299173078  0.01321268358177  173.58353085527
     8        1.5238214566E-03   5.1254955246E-03  5.3472176133E-03  -16.557332714689
     9        1.7869684573E-03   1.2865216655E-03  2.2019069606E-03  -54.248130516652
**** FILE INPUT ****** set xloc=-0.388,0.000,3.750,0.135,0.000,0.000
**** FILE INPUT ****** circ
**** FILE INPUT ****** fit
Polynomial fitting to tabulated values on a line
Component:  BY
Fourier coefficients
   Order       Sine term          Cosine term       Amplitude          Phase
   n            A_n                B_n
     0        0.0                -14157.250146413  14157.2501464134  179.999994991044
     1        4.59369473540686   -7.3243464692022  8.64569734162721  -147.90481907159
     2        0.0909208071963    3.08148213482303  3.08282317696211  -1.6900527787271
     3        -0.0274160580733   -0.6634682665212  0.66403447269017  177.633745858299
     4        8.8498984005E-03   0.4554072930726   0.45549327468735  -1.1132847602393
     5        -4.863599595E-03   -0.01923717737    0.01984246945795  165.811625446259
     6        -3.719449E-05      0.01975871813659  0.01975875314465  0.10785541384169
     7        -1.629066516E-03   -0.0160992561678  0.01618146800722  174.221963737946
     8        1.2800106708E-03   5.1448076077E-03  5.3016481058E-03  -13.971331170828
     9        -3.488141032E-04   -1.419596163E-03  1.4618223366E-03  166.195129273418
**** FILE INPUT ****** set xloc=-0.389,0.000,3.500,0.126,0.000,0.000
**** FILE INPUT ****** circ
**** FILE INPUT ****** fit
Polynomial fitting to tabulated values on a line
Component:  BY
Fourier coefficients
   Order       Sine term          Cosine term       Amplitude          Phase
   n            A_n                B_n
     0        0.0                -14157.445386892  14157.4453868919  179.999994991044
     1        4.59484731534819   -7.3308804992314  8.65184551095159  -147.9213437621
     2        0.08976135010056   3.08318678785693  3.08449312996275  -1.667590859462
     3        -0.0279429687192   -0.6631681869694  0.6637566223467   177.587232005513
     4        0.01073542813791   0.45291977050195  0.4530469820326   -1.3578112388807
     5        -4.362520198E-03   -0.0173890839966  0.01792796209048  165.916472258888
     6        6.0536434893E-04   0.01907923814028  0.01908883951445  -1.8173256545918
     7        -7.661359364E-05   -0.0118161656635  0.01181641403428  179.628506129039
     8        -8.923509692E-04   1.5040448509E-03  1.7488399486E-03  30.6806878528157
     9        6.3773610118E-04   2.4205571508E-03  2.5031588553E-03  -14.76010618008
**** FILE INPUT ****** set xloc=-0.389,0.000,3.250,0.117,0.000,0.000
**** FILE INPUT ****** circ
**** FILE INPUT ****** fit
```

```
Polynomial fitting to tabulated values on a line
Component:  BY
Fourier coefficients
   Order       Sine term         Cosine term       Amplitude         Phase
   n             A_n               B_n
     0        0.0               -14157.633809878  14157.6338098783  179.999994991044
     1        4.59332114366572  -7.3311320543829  8.65124825257295  -147.9307929047
     2        0.09013663357901  3.08202437407107  3.0833421566672   -1.6751901488307
     3        -0.0263842147121  -0.6652081181202  0.66573115234226  177.728657503123
     4        9.9563785219E-03  0.45383025634573  0.45393945746993  -1.2567847792145
     5        -5.985043827E-03  -0.0184083281786  0.01935684106295  161.989254668508
     6        6.1913960906E-04  0.01845808553929  0.01846846652084  -1.9211521197788
     7        -1.872383874E-04  -0.0144471574121  0.01444837068684  179.25747048138
     8        5.0261780246E-04  4.2908390881E-03  4.3201764704E-03  -6.6810331676711
     9        -3.26386608E-04   2.8900869745E-04  4.3595211331E-04  48.4757625854845
**** FILE INPUT ****** set xloc=-0.390,0.000,3.000,0.108,0.000,0.000
**** FILE INPUT ****** circ
**** FILE INPUT ****** fit
Polynomial fitting to tabulated values on a line
Component:  BY
Fourier coefficients
   Order       Sine term         Cosine term       Amplitude         Phase
   n             A_n               B_n
     0        0.0               -14157.800491908  14157.8004919082  179.999994991044
     1        4.59318114323953  -7.337385611849   8.6564739144515   -147.95355455816
     2        0.0897675295642   3.08428952173693  3.08559557675019  -1.667109674529
     3        -0.026530836026   -0.6680585388903  0.66858514539622  177.725783358824
     4        9.5647017181E-03  0.45418679466081  0.45428749483474  -1.2064111990737
     5        -5.636173735E-03  -0.0176201199422  0.01849959678335  162.262004086592
     6        9.2950305856E-04  0.0175873059377   0.01761185129627  -3.0253125968007
     7        8.1319972317E-05  -0.0123243087993  0.01232457708476  -179.62194348869
     8        9.9393819547E-05  2.3132044113E-03  2.3153388045E-03  -2.460372873065
     9        1.6425494694E-03  1.2034491658E-03  2.0362363944E-03  -53.770828078799
**** FILE INPUT ****** set xloc=-0.390,0.000,2.750,0.099,0.000,0.000
**** FILE INPUT ****** circ
**** FILE INPUT ****** fit
Polynomial fitting to tabulated values on a line
Component:  BY
Fourier coefficients
   Order       Sine term         Cosine term       Amplitude         Phase
   n             A_n               B_n
     0        0.0               -14157.961297414  14157.9612974138  179.999994991044
     1        4.59436355380422  -7.3356892020472  8.65566361023558  -147.94096197877
     2        0.08820515618261  3.0843212284509   3.08558221246009  -1.6380933150196
     3        -0.0258214546247  -0.6683273400709  0.66882597213714  177.787419278709
     4        8.5810253354E-03  0.45580979115846  0.45589055672576  -1.0785166542534
     5        -6.280177932E-03  -0.0176308029328  0.0187159249547   160.393848657733
     6        3.1344083317E-04  0.01815089748055  0.01815360362312  -0.9893203114823
     7        -2.249789496E-04  -0.0129389977739  0.01294095355527  179.003855619041
     8        -7.889267808E-04  3.6283742089E-03  3.7131529548E-03  12.2670317995734
     9        6.5836178767E-04  1.6948513252E-04  6.7982751754E-04  -75.563544595283
**** FILE INPUT ****** set xloc=-0.391,0.000,2.500,0.090,0.000,0.000
**** FILE INPUT ****** circ
**** FILE INPUT ****** fit
Polynomial fitting to tabulated values on a line
Component:  BY
Fourier coefficients
   Order       Sine term         Cosine term       Amplitude         Phase
   n             A_n               B_n
     0        0.0               -14158.099915414  14158.099915414   179.999994991044
     1        4.59384926948977  -7.3407164693181  8.65965180556988  -147.9615012498
     2        0.08893745979002  3.0857861185668   3.08706751485831  -1.6509020593249
     3        -0.0267548425349  -0.6707924495322  0.67132580164069  177.715939168142
     4        0.01049672131629  0.45648747661963  0.45660814433051  -1.3172581464491
     5        -5.652394064E-03  -0.0167189139701  0.0176485592327   161.320432965402
     6        -8.149117827E-04  0.01924334431473  0.01926059141431  2.42489678350307
     7        2.169047057E-03   -0.0135107722805  0.01368377626064  -170.87943901934
     8        -1.617269568E-03  4.5585798105E-03  4.8369629669E-03  19.5334057214964
     9        1.113139148E-03   3.934927993E-04   1.1806419211E-03  -70.531583062358
**** FILE INPUT ****** set xloc=-0.391,0.000,2.250,0.081,0.000,0.000
**** FILE INPUT ****** circ
**** FILE INPUT ****** fit
Polynomial fitting to tabulated values on a line
Component:  BY
Fourier coefficients
   Order       Sine term         Cosine term       Amplitude         Phase
   n             A_n               B_n
     0        0.0               -14158.229921005  14158.2299210054  179.999994991044
     1        4.59348194257333  -7.3428029741594  8.66122577202973  -147.9708832483
     2        0.08920707708816  3.08593942744272  3.08722853906998  -1.6558218304191
     3        -0.0266677843158  -0.6708604796545  0.67139031411138  177.72359410274
     4        9.5187455754E-03  0.45528585588289  0.45538535009851  -1.1977189319931
     5        -6.08738523E-03   -0.0165896729785  0.01767126222065  159.849977890529
     6        1.7757830684E-03  0.01846605898737  0.01855124632016  -5.4929407267946
     7        -6.967472893E-04  -0.0128060779173  0.01282501806665  176.885742742182
     8        3.7621976919E-04  2.4385695036E-03  2.4674202193E-03  -8.7703805064909
```

```
     9        7.2699768521E-04  1.8509929804E-03  1.9886429161E-03  -21.442958974965
**** FILE INPUT ****** set xloc=-0.391,0.000,2.000,0.072,0.000,0.000
**** FILE INPUT ****** circ
**** FILE INPUT ****** fit
Polynomial fitting to tabulated values on a line
Component:  BY
Fourier coefficients
   Order       Sine term         Cosine term       Amplitude         Phase
   n             A_n               B_n
     0        0.0               -14158.349412381  14158.3494123807  179.999994991044
     1        4.5952167541058   -7.33868569985    8.65865606306182  -147.94670191283
     2        0.08857929626807  3.08394816200746  3.08522001770968  -1.6452367022222
     3        -0.0258413526389  -0.6696333037337  0.67013173106152  177.790030113328
     4        8.7506703959E-03  0.45649777080371  0.45658163452019  -1.0981763810946
     5        -3.332067883E-03  -0.0184750794974  0.01877315207442  169.776336364181
     6        8.9942119588E-06  0.01972887731915  0.01972887936934  -0.0261206112699
     7        1.0853481562E-03  -0.0153606832615  0.01539897954025  -175.95833308375
     8        5.3559732175E-04  5.3531976682E-03  5.3799246989E-03  -5.7135342471417
     9        -2.816920354E-04  -1.711463046E-03  1.7344901734E-03  170.653404297231
**** FILE INPUT ****** set xloc=-0.392,0.000,1.750,0.063,0.000,0.000
**** FILE INPUT ****** circ
**** FILE INPUT ****** fit
Polynomial fitting to tabulated values on a line
Component:  BY
Fourier coefficients
   Order       Sine term         Cosine term       Amplitude         Phase
   n             A_n               B_n
     0        0.0               -14158.447521735  14158.4475217351  179.999994991044
     1        4.59201094328114  -7.3438513562339  8.6613346111135   -147.98281091678
     2        0.08844519598309  3.087892816178    3.08915920549527  -1.640649949062
     3        -0.0269296217313  -0.6736896931743  0.67422771169382  177.71091054005
     4        8.1642313932E-03  0.45782284204648  0.45789563152946  -1.0216318847588
     5        -5.677209114E-03  -0.0164449313905  0.01739731219937  160.954017731557
     6        -2.007702681E-03  0.01929340761166  0.01939758869868  5.94090702301863
     7        1.0158932713E-03  -0.0132223720605  0.01326134088413  -175.60651196566
     8        -8.259916556E-04  4.4844756493E-03  4.5599105325E-03  10.4362892146395
     9        -1.191943046E-03  8.1568179223E-04  1.4443216443E-03  55.6150108145679
**** FILE INPUT ****** set xloc=-0.392,0.000,1.500,0.054,0.000,0.000
**** FILE INPUT ****** circ
**** FILE INPUT ****** fit
Polynomial fitting to tabulated values on a line
Component:  BY
Fourier coefficients
   Order       Sine term         Cosine term       Amplitude         Phase
   n             A_n               B_n
     0        0.0               -14158.535440175  14158.5354401752  179.999994991044
     1        4.59370161147281  -7.3479062809218  8.6656691148727   -147.98754705618
     2        0.08829171451899  3.09031833192728  3.09157934064428  -1.6365196609548
     3        -0.0258873776498  -0.6728710230927  0.67336882170134  177.796740246677
     4        8.3394359909E-03  0.45655565358896  0.4566318112185   -1.0464471069071
     5        -6.201410618E-03  -0.0152302192824  0.01644436295655  157.844922404432
     6        3.6098896624E-04  0.01900477093102  0.01900819905131  -1.0881823718987
     7        -1.860798307E-03  -0.0124115179058  0.0125502329486   171.473425585328
     8        1.7232603018E-04  3.5192314751E-03  3.5234480891E-03  -2.8033603018034
     9        -2.569554992E-03  1.326350806E-03   2.8916810539E-03  62.6981569308117
**** FILE INPUT ****** set xloc=-0.392,0.000,1.250,0.045,0.000,0.000
**** FILE INPUT ****** circ
**** FILE INPUT ****** fit
Polynomial fitting to tabulated values on a line
Component:  BY
Fourier coefficients
   Order       Sine term         Cosine term       Amplitude         Phase
   n             A_n               B_n
     0        0.0               -14158.612505078  14158.6125050778  179.999994991044
     1        4.59335458762689  -7.3483570758551  8.6658674165915   -147.9910725322
     2        0.08716661233849  3.08699898999652  3.08822939279874  -1.6174129577995
     3        -0.0255816254061  -0.6735309995811  0.67401663700173  177.824868781898
     4        0.01004071950377  0.45556293088043  0.45567356741479  -1.2626086748872
     5        -8.523919668E-03  -0.0158685733779  0.01801301828003  151.757203406424
     6        1.8167954726E-03  0.0166584483141   0.01675722668053  -6.224164066284
     7        -9.235057894E-04  -0.0104802230417  0.01052083351961  174.964161158677
     8        -1.135540423E-03  2.5879058322E-03  2.8260765468E-03  23.6912590931188
     9        -1.412784209E-03  6.0482415734E-05  1.4140782669E-03  87.5486165395428
**** FILE INPUT ****** set xloc=-0.392,0.000,1.000,0.036,0.000,0.000
**** FILE INPUT ****** circ
**** FILE INPUT ****** fit
Polynomial fitting to tabulated values on a line
Component:  BY
Fourier coefficients
   Order       Sine term         Cosine term       Amplitude         Phase
   n             A_n               B_n
     0        0.0               -14158.675670467  14158.6756704671  179.999994991044
     1        4.59203195671465  -7.345664825007   8.66288342371252  -147.98905206858
     2        0.08887865510683  3.08896138342277  3.09023977121691  -1.6481161306756
     3        -0.0242229563737  -0.6728932101017  0.67332906057625  177.938339334603
     4        9.9412757004E-03  0.45332350786646  0.45343249965888  -1.2562812929621
```

```
     5        -5.040079061E-03  -0.0158190456758  0.01660254808864  162.327685436911
     6        1.8318835282E-03  0.0170929423179   0.01719082529561  -6.1171499417005
     7        1.7745276163E-03  -0.013800694504   0.01391431338776  -172.67296525987
     8        -7.506521921E-04  4.1333159689E-03  4.2009260422E-03  10.2933086261372
     9        1.1338622628E-03  1.434817575E-04   1.1429044779E-03  -82.787979256232
**** FILE INPUT ****** set xloc=-0.392,0.000,0.750,0.027,0.000,0.000
**** FILE INPUT ****** circ
**** FILE INPUT ****** fit
Polynomial fitting to tabulated values on a line
Component:  BY
Fourier coefficients
   Order       Sine term         Cosine term       Amplitude         Phase
   n             A_n               B_n
     0        0.0               -14158.723523252  14158.7235232517  179.999994991044
     1        4.59165418830533  -7.3491740008368  8.66565904473268  -148.00346898228
     2        0.09076069046191  3.09131442505941  3.09264650057414  -1.6817153557252
     3        -0.0259928389144  -0.6738921040375  0.67439320545129  177.791122053709
     4        9.8575913419E-03  0.45596591342303  0.4560724573034   -1.2384925697222
     5        -4.419541976E-03  -0.0151676246722  0.01579839199023  163.754930731436
     6        7.1797754072E-04  0.01929099681195  0.01930435312948  -2.1314659650972
     7        2.2312133451E-03  -0.013726874812   0.01390702718396  -170.76768456112
     8        -2.05384079E-03   5.156632008E-03   5.5505959732E-03  21.716953115923
     9        1.5032699322E-03  -5.006958879E-04  1.5844610633E-03  -108.42142641392
**** FILE INPUT ****** set xloc=-0.392,0.000,0.500,0.018,0.000,0.000
**** FILE INPUT ****** circ
**** FILE INPUT ****** fit
Polynomial fitting to tabulated values on a line
Component:  BY
Fourier coefficients
   Order       Sine term         Cosine term       Amplitude         Phase
   n             A_n               B_n
     0        0.0               -14158.758309518  14158.7583095183  179.999994991044
     1        4.59192956806768  -7.3485964259094  8.66531514654737  -147.9999012182
     2        0.08935231707648  3.08952809082879  3.09081990102742  -1.656590818361
     3        -0.0266295586874  -0.6753982659979  0.67592303637975  177.742110326768
     4        0.01005545275263  0.45647640965021  0.45658714907146  -1.2619312031779
     5        -6.422151946E-03  -0.0155860407484  0.01685730410936  157.606124811099
     6        1.6800135034E-03  0.01758545512209  0.01766552227427  -5.4571480680024
     7        -7.222659803E-05  -0.0119697198353  0.01196993774493  179.654270199407
     8        5.052326518E-04   3.5443603157E-03  3.5801885537E-03  -8.1126032700303
     9        -1.904297593E-03  1.8121001434E-03  2.6286985852E-03  46.4211171652486
**** FILE INPUT ****** set xloc=-0.393,0.000,0.250,0.009,0.000,0.000
**** FILE INPUT ****** circ
**** FILE INPUT ****** fit
Polynomial fitting to tabulated values on a line
Component:  BY
Fourier coefficients
   Order       Sine term         Cosine term       Amplitude         Phase
   n             A_n               B_n
     0        0.0               -14158.772537517  14158.7725375174  179.999994991044
     1        4.59416406656883  -7.3545166251955  8.67151995101375  -148.00810937009
     2        0.08838337659155  3.09082433652537  3.09208775757016  -1.6379496765519
     3        -0.0264405351835  -0.6752013633226  0.67571886382839  177.757467855714
     4        9.3848125026E-03  0.45624546506019  0.45634197603738  -1.1783882940148
     5        -4.68288301E-03   -0.0154116260273  0.016107377505    163.098385571593
     6        5.3192865716E-04  0.01891462926517  0.01892210739677  -1.6108819772717
     7        -3.960022787E-04  -0.0135744188693  0.01358019386624  178.32899709517
     8        8.1322045936E-04  4.9826414652E-03  5.0485684591E-03  -9.2695546736925
     9        -1.040430281E-03  4.17813784E-05    1.0412688668E-03  87.7003614429179
**** FILE INPUT ****** set xloc=-0.393,0.000,0.000,0.000,0.000,0.000
**** FILE INPUT ****** circ
**** FILE INPUT ****** fit
Polynomial fitting to tabulated values on a line
Component:  BY
Fourier coefficients
   Order       Sine term         Cosine term       Amplitude         Phase
   n             A_n               B_n
     0        0.0               -14158.779791193  14158.7797911933  179.999994991044
     1        4.58928810387388  -7.3553624138344  8.66965521455183  -148.03840077785
     2        0.09173082194725  3.09333809767548  3.09469790613328  -1.6985692607803
     3        -0.0242591073493  -0.675976485128   0.676411644441    177.94467471087
     4        8.7318785322E-03  0.45292483934065  0.4530090018912   -1.1044609626681
     5        -7.343389514E-03  -0.0165156176733  0.01807459533938  156.028483336488
     6        4.7265315653E-04  0.0180756380031   0.0180818165632   -1.4978647276372
     7        1.823993355E-03   -0.0130811545133  0.01320770817207  -172.06204010168
     8        -8.514853933E-04  1.3851914258E-04  8.6267892512E-04  80.7600967385217
     9        -2.155928109E-03  1.8118474665E-03  2.8161706719E-03  49.9562194788036
**** FILE INPUT ****** end
Opera-3d Post-Processor Version 12.009  complete on 25/May/2008 at 19:52:47
                                                 00:02:31.53 (00:02:12.29 cp)
```

Annex [A2]

```
#! C:\Perl64\bin\perl
my @SinCos025;                                          # this is the array I'm
going to use.  In each 'while' loop, it will be refilled with the list (x, y,
z, theta, phi, psi, cos0, sin0 ... cos9, sin9) and then printed
my $unefois;
$unefois = 0;
while(<>)
{
    @SinCos025=undef;                                         # empties the
array (security)

       if(/\\([^\\]*op3)/ and $unefois==0){    # this block contains what I
want to do only once : print the file name and the column headers
              print "Model:";
              print "\t".$1."\n\n";
              print
"x\ty\tz\ttheta\tphi\tpsi\tCos0\tSin0\tCos1\tSin1\tCos2\tSin2\tCos3\tSin3\tCos
4\tSin4\tCos5\tSin5\tCos6\tSin6\tCos7\tSin7\tCos8\tSin8\tCos9\tSin9\n";
              $unefois = 1;
       }
    next unless /set xloc/;
    if (/(set xloc=(.*))/)              # this searches for the line
containing 'set xloc'
       {
              my $loc=$2;
              ($x,$y,$z,$theta,$phi,$psi)=split(',',$loc);         # this
splits it and assigns its values (x,y,z,theta,phi,psi)  to variables with
corresponding names
              $SinCos025[0]=$x;                # I'm now filling the 6 first
terms of my list
              $SinCos025[1]=$y;
              $SinCos025[2]=$z;
              $SinCos025[3]=$theta;
              $SinCos025[4]=$phi;
              $SinCos025[5]=$psi;
    };
       $_=<>;$_=<>;$_=<>;$_=<>;   # this is used to skip 4 lines in the input
file
       next unless /Component:\s*BY/;
       $_=<>;$_=<>;$_=<>;$_=<>;# now we've found the first line containing
multipole values
       for($i=0;$i<10;$i++)
       {
              ($n,$an,$bn,$amp,$phase)=split;         # $an is sine term, $bn
is cosine
              $ii = 6+2*$i;
              $iii = 6+2*$i + 1;
              $SinCos025[$ii]=$bn;
              $SinCos025[$iii]=$an;                           # this loop fills
the items #6 (it's actually the 7th)  to #25 of my list
              $_=<> unless $i==9;
       }
       foreach $SinCos025 (@SinCos025) {print "$SinCos025\t"};     # actually
prints the line
       print "\n";
}
# additionnal column 'foot' headers (may help for long files):
print
"x\ty\tz\ttheta\tphi\tpsi\tCos0\tSin0\tCos1\tSin1\tCos2\tSin2\tCos3\tSin3\tCos
4\tSin4\tCos5\tSin5\tCos6\tSin6\tCos7\tSin7\tCos8\tSin8\tCos9\tSin9\n";
```

Annex [A3]

```
ACTIVATE CASE=1 MODELSYMMETRY=DATABASE | LOAD
SELECT ACTION=DEFAULT | SELECT ACTION=SELECT OPTION=SURFACES |
THREED OPTION=GETVIEW | THREED OPTION=SETVIEW ROTX=-90 ROTY=0.01
ROTZ=0.01 SIZE=100 PERSPECTIVE=NO
SET FIELD=NODAL COIL=NODAL
set XLOCAL=0,YLOCAL=0,ZLOCAL=0,PLOCAL=0,TLOCAL=0,SLOCAL=0
CIRCLE RADIUS=1 TH1=0 TH2=360 ZC=0 NP=60 | PLOT FILE=TEMP COMPONENT=By
FIT TYPE=FOURIER FILE=TEMP COMP=By ORDER=10 PRINT=YES
set xloc=1.374,0.000,74.981,2.699,0.000,0.000
circ
fit
set xloc=1.362,0.000,74.731,2.690,0.000,0.000
circ
fit
set xloc=1.350,0.000,74.481,2.681,0.000,0.000
circ
fit
set xloc=1.338,0.000,74.232,2.672,0.000,0.000
circ
fit
set xloc=1.327,0.000,73.982,2.663,0.000,0.000
circ
fit
set xloc=1.315,0.000,73.732,2.654,0.000,0.000
circ
fit
set xloc=1.304,0.000,73.482,2.645,0.000,0.000
circ
fit
set xloc=1.292,0.000,73.232,2.636,0.000,0.000
circ
fit
set xloc=1.281,0.000,72.983,2.627,0.000,0.000
circ
fit
set xloc=1.269,0.000,72.733,2.618,0.000,0.000
circ
fit
set xloc=1.258,0.000,72.483,2.609,0.000,0.000
circ
fit
set xloc=1.246,0.000,72.233,2.600,0.000,0.000
circ
fit
set xloc=1.235,0.000,71.984,2.591,0.000,0.000
circ
fit
set xloc=1.224,0.000,71.734,2.582,0.000,0.000
circ
fit
set xloc=1.213,0.000,71.484,2.573,0.000,0.000
circ
fit
set xloc=1.201,0.000,71.234,2.564,0.000,0.000
circ
fit
set xloc=1.190,0.000,70.985,2.555,0.000,0.000
circ
```

```
fit
set xloc=1.179,0.000,70.735,2.546,0.000,0.000
circ
fit
set xloc=1.168,0.000,70.485,2.537,0.000,0.000
circ
fit
set xloc=1.157,0.000,70.235,2.528,0.000,0.000
circ
fit
set xloc=1.146,0.000,69.985,2.519,0.000,0.000
circ
fit

...
```

For paper economy reasons this file only presents the first 5 cm and the last 5 cm of the trajectory that the circle along which the field is evaluated in the model follows.

```
...

set xloc=-0.385,0.000,5.001,0.180,0.000,0.000
circ
fit
set xloc=-0.385,0.000,4.751,0.171,0.000,0.000
circ
fit
set xloc=-0.386,0.000,4.501,0.162,0.000,0.000
circ
fit
set xloc=-0.387,0.000,4.250,0.153,0.000,0.000
circ
fit
set xloc=-0.388,0.000,4.000,0.144,0.000,0.000
circ
fit
set xloc=-0.388,0.000,3.750,0.135,0.000,0.000
circ
fit
set xloc=-0.389,0.000,3.500,0.126,0.000,0.000
circ
fit
set xloc=-0.389,0.000,3.250,0.117,0.000,0.000
circ
fit
set xloc=-0.390,0.000,3.000,0.108,0.000,0.000
circ
fit
set xloc=-0.390,0.000,2.750,0.099,0.000,0.000
circ
fit
set xloc=-0.391,0.000,2.500,0.090,0.000,0.000
circ
fit
set xloc=-0.391,0.000,2.250,0.081,0.000,0.000
circ
fit
set xloc=-0.391,0.000,2.000,0.072,0.000,0.000
circ
fit
```

```
set xloc=-0.392,0.000,1.750,0.063,0.000,0.000
circ
fit
set xloc=-0.392,0.000,1.500,0.054,0.000,0.000
circ
fit
set xloc=-0.392,0.000,1.250,0.045,0.000,0.000
circ
fit
set xloc=-0.392,0.000,1.000,0.036,0.000,0.000
circ
fit
set xloc=-0.392,0.000,0.750,0.027,0.000,0.000
circ
fit
set xloc=-0.392,0.000,0.500,0.018,0.000,0.000
circ
fit
set xloc=-0.393,0.000,0.250,0.009,0.000,0.000
circ
fit
set xloc=-0.393,0.000,0.000,0.000,0.000,0.000
circ
fit
end
```

```
Node: CASNRUIZ. Processor: EM64T/x64. System: Windows XP Professional
x64 Edition (Service Pack 2)


_____________________________________________________________________
_____
 |
|
 | Opera-3d Analysis version 12.009       started on 01/May/2008 at
16:01:52 |

|_____________________________________________________________________
______|


 Opening database                         complete 00:00:00.09
(00:00:00.03 cp)

 Simulation 1                              started at 16:01:55
 Opening database ...riFull\Full_abh_jb14kG_05Current.op3, simulation
number 1 on 01/May/2008 at 16:01:55


_____________________________________________________________________
_____________________________________________________

    DETAILS OF SIMULATION
    ---------------------

    TOSCA Magnetostatic analysis

    File: Full_abh_jb14kG_05Current.op3 simulation:  1
    Created on: 01/May/2008 16:00:09
    In Directory: C:\Documents and Settings\nruiz\My
Documents\TOSCA\Spoiling\abh_jb14kG\abh_jb14kG pole swaps
tests\OriFull\
    By Machine: Node: CASNRUIZ. Processor: EM64T/x64. System: Windows.
version XP Professional x64 Edition (Service Pack 2)
    Log Files: Opera3d_Modeller_9.log/lp
    Simulation created using: Opera-3d/Modeller Version 12.009
    User did not enter a title

    Mixed CGS units

    1 Biot-Savart conductor (current densities in A cm**-2):
        1 Racetrack
        Current Densities: 510.0
    Adaptive RHS integrals
    Drive sets and functions
    COND1            : Coil drive type Constant
                       Scaling factor: 0.5

    Boundary Conditions: TANGMAGN

    Non linear iteration data
    Newton-Raphson Iterations
    Maximum Iterations: 40
    Tolerance: 1.0E-03
    No periodicity conditions have been defined

    Materials defined:
    AIR
    JLAB
      Isotropic permeability: M:/opera/shared/JLab S-R.bh (3763.179)

    7934939 nodes in the model
    11230468 edges in the model
```

```
    Mixed linear and quadratic tetrahedral elements
    4275047 linear tetrahedra
    5346565 quadratic tetrahedra
```

```
 Loading problem description             complete 00:00:16.18
(00:00:14.60 cp)
 Setting scalar potential to 0 at node 1 at (-17.13297,149.56413,0.0
) [cm]
 Checking periodicity transformations
 Checking connectivity of potential regions:
  2 automatic potential cuts have been added.
 Preparing data                          complete 00:04:14.63
(00:04:08.15 cp)
 Problem size information
 ------------------------
 Number of elements  : 9621612
 Number of nodes     : 7934939
 Number of equations : 7752319
 Number of non-zeros : 109689916
 Forming Matrix Sparsity                 complete 00:01:33.82
(00:01:21.14 cp)
 Selecting coil field calculations       complete 00:00:37.29
(00:00:37.04 cp)

 Coil set with drive label COND1
 Calculating coil fields at 947415 nodes
   Coil fields computed at 94741 nodes
   Coil fields computed at 189482 nodes
   Coil fields computed at 284223 nodes
   Coil fields computed at 378964 nodes
   Coil fields computed at 473705 nodes
   Coil fields computed at 568446 nodes
   Coil fields computed at 663187 nodes
   Coil fields computed at 757928 nodes
   Coil fields computed at 852669 nodes
   Coil fields computed at 947410 nodes
 Calculating nodal coil fields           complete 00:06:21.78
(00:06:16.29 cp)

 Coil set with drive label COND1
 Calculating line integrals along 140939 edges
   Coil field line integrals computed along 14093 edges
   Coil field line integrals computed along 28186 edges
   Coil field line integrals computed along 42279 edges
   Coil field line integrals computed along 56372 edges
   Coil field line integrals computed along 70465 edges
   Coil field line integrals computed along 84558 edges
   Coil field line integrals computed along 98651 edges
   Coil field line integrals computed along 112744 edges
   Coil field line integrals computed along 126837 edges
   Coil field line integrals computed along 140930 edges
 Total number of field calculations: 318231
 Average number of field calculations per edge: 2.2579
 Calculating edge integral coil fields   complete 00:01:57.89
(00:01:56.14 cp)

 Coil set with drive label COND1
  DSLUCG iterations:    1614 Relative change= 0.99230E-12
 Error in nodal potential jump calculation: 1.3506E-05%
 Calculating nodal potential jump values complete 00:01:52.98
(00:01:51.35 cp)

 Coil set with drive label COND1
 Calculating face integrals of Nodal WH.n over 121642 faces
   Coil field integrals computed over 12164 faces
```

```
   Coil field integrals computed over 24328 faces
   Coil field integrals computed over 36492 faces
   Coil field integrals computed over 48656 faces
   Coil field integrals computed over 60820 faces
   Coil field integrals computed over 72984 faces
   Coil field integrals computed over 85148 faces
   Coil field integrals computed over 97312 faces
   Coil field integrals computed over 109476 faces
   Coil field integrals computed over 121640 faces
 Total number of field calculations: 851494
 Average number of field calculations per face: 7.0
 Calculating face integral coil fields   complete 00:05:23.00
(00:05:18.14 cp)
 Evaluating coil field calculations      complete 00:15:45.51
(00:15:31.67 cp)
 Initial residual: 51325575.

 Nonlinear iteration 1                    started at 16:29:13
 Simple nonlinear update
  DSLUCG iterations:    1071 Relative change= 0.99336E-08
 Iterative matrix solution               complete 00:53:46.51
(00:52:21.56 cp)
 Residual: 918.042188, relaxation factor: 1.0
 Relaxing solution change                complete 00:02:46.46
(00:02:38.42 cp)
 Nonlinear iteration 1                   complete 00:56:34.96
(00:55:01.96 cp)

 Nonlinear iteration 2                    started at 17:25:48
 Newton-Raphson nonlinear update
  DSLUCG iterations:     499 Relative change= 0.51251E-06
 Iterative matrix solution               complete 00:27:10.12
(00:26:30.60 cp)
 Residual: 1161.05011, relaxation factor: 0.0625
 Convergence indicators (Changes): 1.188E-03, 0.7129258 (target 1.0E-
03  )
 Relaxing solution change                complete 00:13:31.27
(00:13:10.15 cp)
 Nonlinear iteration 2                   complete 00:43:40.33
(00:42:36.01 cp)

 Nonlinear iteration 3                    started at 18:09:29
 Simple nonlinear update
  DSLUCG iterations:     375 Relative change= 0.94291E-08
 Iterative matrix solution               complete 00:18:02.80
(00:17:34.84 cp)
 Residual: 1216.13381, relaxation factor: 0.0625
 Convergence indicators (Changes): 6.653E-04, 0.1579107 (target 1.0E-
03  )
 Relaxing solution change                complete 00:18:28.10
(00:18:00.89 cp)
 Nonlinear iteration 3                   complete 00:36:32.87
(00:35:37.68 cp)

 Nonlinear iteration 4                    started at 18:46:02
 Newton-Raphson nonlinear update
 Jacobian terms relaxed 0.25
  DSLUCG iterations:     459 Relative change= 0.54109E-06
 Iterative matrix solution               complete 00:24:50.53
(00:24:14.12 cp)
 Residual: 1288.01111, relaxation factor: 0.0625
 Convergence indicators (Changes): 7.163E-04, 0.2656289 (target 1.0E-
03  )
 Relaxing solution change                complete 00:18:27.83
(00:17:51.71 cp)
 Nonlinear iteration 4                   complete 00:45:49.11
(00:44:33.56 cp)

 Nonlinear iteration 5                    started at 19:31:51
```

```
 Newton-Raphson nonlinear update
 Jacobian terms relaxed 0.469519
  DSLUCG iterations:     469 Relative change= 0.57058E-06
 Iterative matrix solution               complete 00:19:37.50
(00:19:02.87 cp)
 Residual: 1382.28799, relaxation factor: 0.0625
 Convergence indicators (Changes): 7.712E-04, 0.3138164 (target 1.0E-
03  )
 Relaxing solution change                complete 00:12:47.32
(00:10:46.79 cp)
 Nonlinear iteration 5                   complete 00:34:59.68
(00:32:18.12 cp)

 Nonlinear iteration 6                    started at 20:06:51
 Newton-Raphson nonlinear update
 Jacobian terms relaxed 0.422676
  DSLUCG iterations:     466 Relative change= 0.58270E-06
 Iterative matrix solution               complete 00:18:34.14
(00:18:16.92 cp)
 Residual: 1472.25805, relaxation factor: 0.0625
 Convergence indicators (Changes): 7.257E-04, 0.4191024 (target 1.0E-
03  )
 Relaxing solution change                complete 00:15:21.17
(00:15:06.65 cp)
 Nonlinear iteration 6                   complete 00:36:23.60
(00:35:50.06 cp)

 Nonlinear iteration 7                    started at 20:43:14
 Simple nonlinear update
  DSLUCG iterations:     373 Relative change= 0.97914E-08
 Iterative matrix solution               complete 00:14:53.17
(00:14:39.64 cp)
 Residual: 1532.67238, relaxation factor: 0.0625
 Convergence indicators (Changes): 5.734E-04, 0.2428453 (target 1.0E-
03  )
 Relaxing solution change                complete 00:15:21.18
(00:15:06.78 cp)
 Nonlinear iteration 7                   complete 00:30:16.25
(00:29:48.31 cp)

 Nonlinear iteration 8                    started at 21:13:30
 Newton-Raphson nonlinear update
  DSLUCG iterations:     507 Relative change= 0.58644E-06
 Iterative matrix solution               complete 00:20:13.05
(00:19:53.83 cp)
 Residual: 1841.47389, relaxation factor: 0.0625
 Convergence indicators (Changes): 1.074E-03, 1.1762944 (target 1.0E-
03  )
 Relaxing solution change                complete 00:13:10.13
(00:12:57.45 cp)
 Nonlinear iteration 8                   complete 00:35:51.51
(00:35:17.81 cp)

 Nonlinear iteration 9                    started at 21:49:22
 Newton-Raphson nonlinear update
 Jacobian terms relaxed 0.411812
  DSLUCG iterations:     466 Relative change= 0.62560E-06
 Iterative matrix solution               complete 00:18:37.17
(00:18:20.36 cp)
 Residual: 2137.60026, relaxation factor: 2.0
 Convergence indicators (Changes): 6.535E-04, 0.7008913 (target 1.0E-
03  )
 Relaxing solution change                complete 00:13:07.97
(00:12:57.15 cp)
 Nonlinear iteration 9                   complete 00:34:13.46
(00:33:44.01 cp)

 Nonlinear iteration 10                   started at 22:23:36
 Newton-Raphson nonlinear update
```

```
 Jacobian terms relaxed 0.661812
  DSLUCG iterations:     955 Relative change= 0.84330E-06
 Iterative matrix solution               complete 00:37:53.64
(00:37:20.73 cp)
 Residual: 2166.07792, relaxation factor: 0.0625
 Convergence indicators (Changes): 3.337E-04, 1.0089306 (target 1.0E-
03  )
 Relaxing solution change                complete 00:21:55.24
(00:21:35.42 cp)
 Nonlinear iteration 10                  complete 01:02:18.97
(01:01:22.66 cp)

 Nonlinear iteration 11                   started at 23:25:55
 Newton-Raphson nonlinear update
 Jacobian terms relaxed 0.912046
  DSLUCG iterations:    1028 Relative change= 0.85639E-06
 Iterative matrix solution               complete 00:40:51.46
(00:40:14.18 cp)
 Residual: 2287.02397, relaxation factor: 2.0
 Convergence indicators (Changes): 5.793E-04, 1.8099201 (target 1.0E-
03  )
 Relaxing solution change                complete 00:13:08.50
(00:12:57.60 cp)
 Nonlinear iteration 11                  complete 00:56:30.22
(00:55:38.41 cp)

 Nonlinear iteration 12                   started at 00:22:25
 Newton-Raphson nonlinear update
 Jacobian terms relaxed 0.897612
  DSLUCG iterations:    1042 Relative change= 0.11989E-05
 Iterative matrix solution               complete 00:41:22.56
(00:40:44.11 cp)
 Residual: 848.204579, relaxation factor: 1.0
 Convergence indicators (Changes): 7.087E-04, 0.585946  (target 1.0E-
03  )
 Relaxing solution change                complete 00:02:11.53
(00:02:09.73 cp)
 Nonlinear iteration 12                  complete 00:46:02.47
(00:45:20.40 cp)

 Nonlinear iteration 13                   started at 01:08:27
 Newton-Raphson nonlinear update
  DSLUCG iterations:     491 Relative change= 0.45054E-05
 Iterative matrix solution               complete 00:19:34.78
(00:19:16.14 cp)
 Residual: 180.909221, relaxation factor: 1.0
 Convergence indicators (Changes): 3.971E-04, 0.7704239 (target 1.0E-
03  )
 Relaxing solution change                complete 00:02:11.56
(00:02:09.76 cp)
 Nonlinear iteration 13                  complete 00:24:14.69
(00:23:52.45 cp)

 Nonlinear iteration 14                   started at 01:32:42
 Newton-Raphson nonlinear update
  DSLUCG iterations:     412 Relative change= 0.18134E-04
 Iterative matrix solution               complete 00:16:26.10
(00:16:11.29 cp)
 Residual: 12.749083 , relaxation factor: 1.0
 Convergence indicators (Changes): 2.829E-05, 0.0614732 (target 1.0E-
03  )
 Relaxing solution change                complete 00:02:11.53
(00:02:09.71 cp)
 Nonlinear iteration 14                  complete 00:21:05.97
(00:20:47.56 cp)

 Nonlinear iteration 15                   started at 01:53:48
 Newton-Raphson nonlinear update
  DSLUCG iterations:     382 Relative change= 0.99830E-04
```

```
 Iterative matrix solution               complete 00:15:15.55
(00:15:00.82 cp)
 Residual: 0.18251914, relaxation factor: 1.0
 Convergence indicators (Changes): 1.149E-06, 1.604E-03 (target 1.0E-
03  )
 Relaxing solution change                complete 00:02:11.56
(00:02:09.76 cp)
 Nonlinear iteration 15                  complete 00:19:55.53
(00:19:37.21 cp)

 Nonlinear iteration 16                   started at 02:13:44
 Newton-Raphson nonlinear update
  DSLUCG iterations:     603 Relative change= 0.94756E-04
 Iterative matrix solution               complete 00:24:01.35
(00:23:38.78 cp)
 Residual: 3.2401E-04, relaxation factor: 1.0
 Convergence indicators (Changes): 7.914E-07, 1.932E-04 (target 1.0E-
03  )
 Relaxing solution change                complete 00:02:11.62
(00:02:09.78 cp)
 Nonlinear iteration 16                  complete 00:28:41.29
(00:28:15.07 cp)


 Calculating nodal fields                 started
 Generating nodal H fields               complete 00:02:12.15
(00:02:10.34 cp)
 Enforcing H fields on boundaries        complete 00:00:53.79
(00:00:53.76 cp)
 Adjusting midside nodal values          complete 00:02:09.49
(00:02:05.90 cp)
 Generating nodal B fields               complete 00:02:12.85
(00:02:11.03 cp)
 Estimated error in B Field: RMS = 5.95158 %, Weighted RMS = 0.491265%
 Calculating error estimate              complete 00:04:31.71
(00:04:28.10 cp)
 Calculating nodal fields                complete 00:12:00.29
(00:11:49.42 cp)
 Simulation 1                            complete at 02:54:34
                                                     10:52:39.07
(10:37:58.52 cp)


_____________________________________________________________________
_______
 |
|
 | Opera-3d Analysis version 12.009      complete on 02/May/2008 at
02:54:34   |
 |                                                   10:52:42.47
(10:37:58.60 cp) |

|_____________________________________________________________________
________|
```